



Cytoprotective effects of α -linolenic acid, eicosapentaenoic acid, docosahexaenoic acid, oleic acid and α -tocopherol on 7-ketocholesterol – Induced oxiaoptophagy: Major roles of PI3-K / PDK-1 / Akt signaling pathway and glutathione peroxidase activity in cell rescue

Aline Yammine^{a,b}, Imen Ghzaïel^{a,c,f}, Vivien Pires^{a,g}, Amira Zarrouk^{c,d}, Omar Kharoubi^e, H  l  ne Greige-Gerges^b, Lizette Auezova^b, G  rard Lizard^{a,*}, Anne Vejux^{a,g,*}

^a Team 'Biochemistry of the Peroxisome, Inflammation and Lipid Metabolism' EA7270 / Inserm, University of Bourgogne, 21000 Dijon, France

^b Bioactive Molecules Research Laboratory, Doctoral School of Sciences and Technologies, Faculty of Sciences, Lebanese University, Fanar, Jdeidet P.O. Box 90656, Lebanon

^c Lab-NAFS 'Nutrition-Functional Food & Vascular Health', Faculty of Medicine, University of Monastir, LR12ES05, Monastir 5000, Tunisia

^d Faculty of Medicine, University of Sousse, Sousse 4000, Tunisia

^e University Oran 1 ABB: Laboratory of Experimental Biotoxicology, Biodepollution and Phytoremediation, Faculty of Life and Natural Sciences, Oran, Algeria

^f Universit   Clermont Auvergne, Clermont Auvergne INP, CNRS, Institut Pascal, F-63000 Clermont-Ferrand, France

^g Centre des Sciences du Go  t et de l'Alimentation, CNRS, INRAE, Institut Agro, Universit   de Bourgogne, F-21000 Dijon, France

ARTICLE INFO

Keywords:

7-ketocholesterol
 α -tocopherol
 Eicosapentaenoic acid
 α -linolenic acid
 Oleic acid
 glutathione peroxidase
 Oxiaoptophagy

ABSTRACT

On murine N2a cells, 7-ketocholesterol induced an oxiaoptophagic mode of cell death characterized by oxidative stress (reactive oxygen species overproduction on whole cells and at the mitochondrial level; lipid peroxidation), apoptosis induction (caspase-9, -3 and -7 cleavage, PARP degradation) and autophagy (increased ratio LC3-II / LC3-I). Oxidative stress was strongly attenuated by diphenyleneiodonium chloride which inhibits NAD(P)H oxidase. Mitochondrial and peroxisomal morphological and functional changes were also observed. Down regulation of PDK1 / Akt signaling pathways as well as of GSK3 / Mcl-1 and Nrf2 pathways were simultaneously observed in 7-ketocholesterol-induced oxiaoptophagy. These events were prevented by α -linolenic acid, eicosapentaenoic acid, docosahexaenoic acid, oleic acid and α -tocopherol. The inhibition of the cytoprotection by LY-294002, a PI3-K inhibitor, demonstrated an essential role of PI3-K in cell rescue. The rupture of oxidative stress in 7-ketocholesterol-induced oxiaoptophagy was also associated with important modifications of glutathione peroxidase, superoxide dismutase and catalase activities as well as of glutathione peroxidase-1, superoxide dismutase-1 and catalase level and expression. These events were also counteracted by α -linolenic acid, eicosapentaenoic acid, docosahexaenoic acid, oleic acid and α -tocopherol. The inhibition of the cytoprotection by mercaptosuccinic acid, a glutathione peroxidase inhibitor, showed an essential role of this enzyme in cell rescue. Altogether, our data support that the reactivation of PI3-K and glutathione peroxidase activities by α -linolenic acid, eicosapentaenoic acid, docosahexaenoic acid, oleic acid and α -tocopherol are essential to prevent 7KC-induced oxiaoptophagy.

Introduction

Derivatives of cholesterol oxidation, called oxysterols, are molecules that are implicated in the development of many diseases especially age-related diseases such as cardiovascular, neurodegenerative, and eye diseases, osteoporosis, sarcopenia, and some cancers (breast and

prostate cancers) (Zarrouk et al., 2014; Gargiulo et al., 2016). Oxysterols, present in vivo, detected in biological fluids and tissues, can be produced endogenously, synthesis by auto-oxidation and/or enzymatically (Brzeska et al., 2016; Muteberezzi et al., 2016), or provided by the diet (Sabolov   et al., 2017). Among the numerous food products, eggs, dried egg powder often used in a large number of commercial products

* Corresponding authors.

E-mail addresses: gerard.lizard@u-bourgogne.fr (G. Lizard), anne.vejux@u-bourgogne.fr (A. Vejux).

<https://doi.org/10.1016/j.crttox.2024.100153>

Received 16 November 2023; Received in revised form 23 January 2024; Accepted 5 February 2024

Available online 8 February 2024

2666-027X/   2024 The Author(s). Published by Elsevier B.V. This is an open access article under the CC BY-NC-ND license (<http://creativecommons.org/licenses/by-nc-nd/4.0/>).

(Boselli et al., 2001), milk powder found in children's products (Przygowski et al., 2000), clarified butter (or ghee), cheeses, dairy products, red meat (beef, pork, veal), ham, liver, kidneys, dried or canned fish (cod, anchovies, herrings) are included (Poli et al., 2022). All cholesterol-containing products are subject to oxidation, especially processed foods often subjected to dehydration, radiation, high temperatures, and/or long-term storage in the presence of oxygen (Leonarduzzi et al., 2002; Yan, 1999).

There is now lot of evidence supporting that oxysterols formed by autoxidation such as 7-ketocholesterol (7KC) and 7 β -hydroxycholesterol (7 β -OHC) are implicated in the atheromatous plaque formation which contribute to several cardiovascular diseases and stroke (Poli et al., 2013; Wang et al., 2017). 7KC has also been found at increased level in patients with neurodegenerative diseases such as X-linked adrenoleukodystrophy (X-ALD) (Nury et al., 2017), Alzheimer's disease (Choroszyński et al., 2022; Mahalakshmi et al., 2021), multiple sclerosis (McComb et al., 2021), and Parkinson's disease (Griffiths et al., 2021). In patients with age-related macular degeneration (AMD), high 7KC levels are also present in lipid deposits called drusen which are localized between the Bruch membrane and the basement membrane of retinal pigment epithelial cells (Malvite et al., 2006; Rodríguez and Larrayoz, 2010; Rodríguez et al., 2014). The cytotoxic properties of 7KC and 7 β -OHC are exerted through stimulation of oxidative stress, activation of death pathways (apoptosis, autophagy) and cytokinetic and non-cytokinetic inflammation (Vejux et al., 2020). The ability of 7KC and 7 β -OHC to trigger a rupture of the RedOx status, and to induce apoptosis associated with several criteria of autophagy is defined as oxia-poptophagy (OXIdative stress + APOPTosis + autoPHAGY) (Nury et al., 2020). Noteworthy, oxia-poptophagy has also been reported in the presence of 24S-hydroxycholesterol (24S-OHC) which can be increased in the brain of Alzheimer's patients at early stages of the disease (Leoni and Caccia, 2013). With the significant increase in lifespan observed since the mid-20th century, the frequency of age-related diseases is increasing with economic and social repercussions. Preventing these diseases and identifying molecules to better treat them is therefore an important challenge. Interestingly, several molecules present at high levels in the Mediterranean diet such as docosahexaenoic acid (DHA, C22:6n-3), eicosapentaenoic acid (EPA, C20:5n-3), α -linolenic acid (ALA, C18:3n-3) and oleic acid (OA, C18:1n-9), as well as Mediterranean oils (olive and argan oils) are able to strongly reduce 7KC- and 7 β -OHC-induced oxia-poptophagy (Vejux et al., 2020; Nury et al., 2021; Rezig et al., 2022). In human nerve SK-N-BE cells treated with 7KC or 7 β -OHC, DHA inhibits 24S-OHC-induced intracellular Ca²⁺ rise and also reduces reactive oxygen species (ROS) overproduction, and apoptosis characterized by condensation and/or fragmentation of the nuclei (Zarrouk et al., 2015). In 158 N murine oligodendrocytes, DHA also counteracts 7KC-, 7 β -OHC- and 24S-OHC-induced oxia-poptophagy characterized by a decrease of cell proliferation, a drop of mitochondrial activity, an overproduction of ROS revealed by staining with dihydroethidium and dihydrorhodamine 123, caspase-3 activation, PARP degradation, reduced expression of Bcl-2, condensation and/or fragmentation of the nuclei, which are biomarkers of oxidative stress and apoptosis, and conversion of microtubule-associated protein light chain 3 (LC3-I) to LC3-II, which is a characteristic of autophagy (Nury et al., 2015). Additionally, in BV-2 murine microglial cells, both OA and DHA attenuate 7KC toxicity characterized by cell growth inhibition, mitochondrial dysfunctions, ROS overproduction, lipid peroxidation, increased plasma membrane permeability, modification of plasma membrane fluidity, nuclei condensation and/or fragmentation and caspase-3 activation, which are apoptotic characteristics, and an increased LC3-II/LC3-I ratio, a criterion of autophagy (Debbabi et al., 2017). Cytoprotective effects of ω 3 and ω 9 unsaturated fatty acids (ALA, EPA, DHA and OA) have also been shown against 7KC-induced cell death in N2a murine nerve cells: attenuation of 7KC-induced ROS overproduction, drop of mitochondrial transmembrane potential ($\Delta\Psi_m$), and increased plasma membrane permeability (Yammine et al., 2020).

Currently, the cytoprotective effects of major compounds of the Mediterranean diet (α -tocopherol, ω 3 and ω 9 unsaturated fatty acids) against 7KC-induced oxia-poptophagy are well established on different cell lines from different types and species (Vejux et al., 2020; Nury et al., 2021; Brahmi et al., 2019). Consequently, these data reinforce the interest of functional foods enriched in α -tocopherol, ω 3 and ω 9 unsaturated fatty acids to prevent the toxicity of 7KC often present at high levels in several processed foods and increased in the biological fluids and tissues of patients with age-related diseases. However, now, the effects of ω 3 (ALA, EPA, DHA) and ω 9 (OA) unsaturated fatty acids on 7KC-induced oxia-poptophagy are still not well known, and the cell targets involved in their cytoprotective activities are unknown. In the present study, murine neuronal N2a cells were used as previously described to establish the ability of polyphenols, ALA, EPA, DHA and α -tocopherol to prevent 7KC-induced cell death (Yammine et al., 2020). On N2a cells, we studied: a) the ability of 7KC to induce mitochondrial and peroxisomal changes associated with oxia-poptophagy; b) the pre-mitochondrial signalling pathways associated with this type of cell death (PI3-K / PDK-1 / Akt / GSK3 / Mcl-1); c) the Nrf2 signalling pathway involved in the antioxidant response and d) the cytoprotective activity of ALA, EPA, DHA and α -tocopherol, and e) we determined the cell targets associated with the cytoprotection.

Materials and methods

Cell culture and treatments

The mouse neuro-2a (N2a) neuroblastoma cells (ref: CCL-131; American Type Culture Collection (ATCC), Manassas, VA, USA) were grown in Dulbecco's modified Eagle medium (DMEM, Lonza, Amboise, France) containing 10 % (v/v) heat-inactivated fetal bovine serum (FBS) (Pan Biotech, Aidenbach, Germany) (30 min, 56 °C) and 1 % (v/v) of penicillin (100 U/mL) / streptomycin (100 mg/mL) (Pan Biotech). N2a cells were maintained at 37 °C in a humidified atmosphere (5 % CO₂, 95 % air) and passaged twice a week. N2a cells were seeded at a density of 120,000 cells per 6-well plates containing 2 mL of culture medium with 10 % FBS, or at a density of 50,000 cells per 24-well plates containing 0.5 mL of culture medium with 10 % FBS (FALCON, Becton Dickinson, Le Pont de Claix, France) or in Petri dishes (100 mm diameter, FALCON) at 30,000 cells/cm². These growing conditions were used to assess the ability of fatty acids (α -linolenic acid (ALA/C18:3n-3); eicosapentaenoic acid (EPA/C20:5n-3); docosahexaenoic acid (DHA, C22:6n-3) and oleic acid (OA, C18:1n-9)) to counteract the cytotoxicity induced by 7-ketocholesterol (7KC). 7KC (ref: 700015P) and fatty acids (ALA (ref: L2376), DHA (ref: D2534), and OA (ref: O1008)) were from Sigma-Aldrich (St Quentin-Fallavier, France) whereas EPA (ref: 10417-94-4) was from Enzo Life Sciences (Villeurbanne, France). The stock solution of 7KC was realized at 800 μ g/mL (2 mM) in absolute ethanol (EtOH; Carlo Erba Reagents, Val de Reuil, France) plus culture medium (800 μ g of 7KC, 50 μ L of absolute ethanol and 950 μ L of culture medium). The 7KC stock solution was stored at 4 °C. The stock solutions of fatty acids (ALA, DHA, OA: 50 mM) or (EPA: 200 mM) were prepared in absolute ethanol and stored at -20 °C. For all experiments, the cells were previously cultured for 24 h, then the medium was removed and replaced by culture medium containing the fatty acids with or without 7KC (time of treatment 48 h). To determine the effects on cell viability, fatty acids (ALA, EPA, DHA and OA) were used at concentrations ranging from 1.5 to 200 μ M. The concentration chosen for 7KC, based on the FDA cell viability assay, corresponds to the 50 % inhibiting concentration (IC50) (Supplementary Fig. 1A). The concentrations chosen for fatty acids, when used with 7KC, is 25 μ M and correspond to a concentration without effect on cell viability (Supplementary Fig. 1B). As a positive cytoprotective control, α -tocopherol was chosen and used at the highest non-toxic concentration (400 μ M) tested on N2a cells and as previously used on 158 N cells to inhibit 7KC-induced toxicity (Ragot et al., 2013); α -tocopherol (ref: T3251; Sigma-Aldrich) stock solution was prepared at 80 mM in

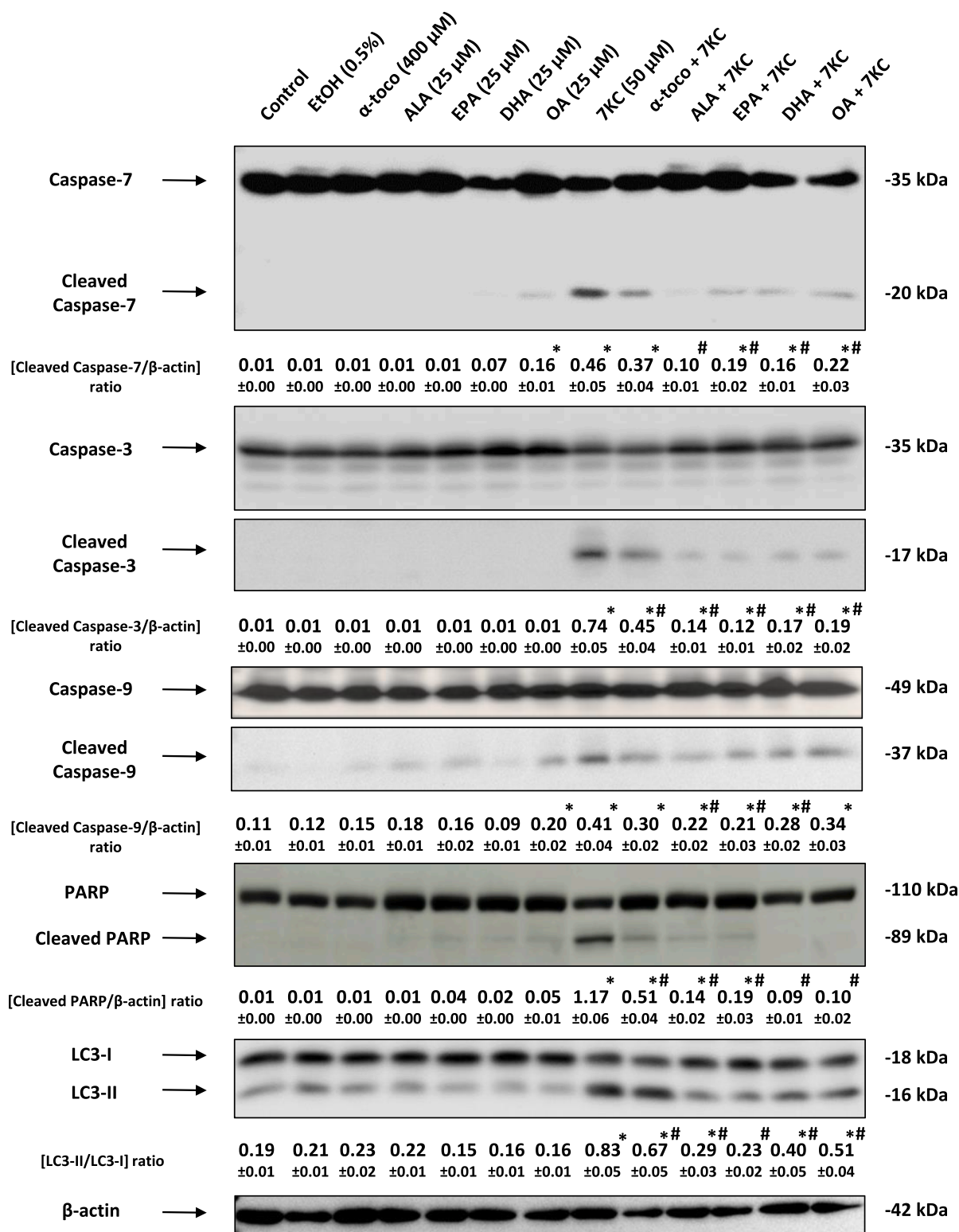


Fig. 1. Effect of α -linolenic acid, eicosapentaenoic acid, docosahexaenoic acid, oleic acid and α -tocopherol on 7KC-induced apoptosis and autophagy: identification of cleaved caspase-3, -7, -9 and PARP, and activation of LC3-I into LC3-II by western blotting. N2a cells were cultured with or without 7-ketocholesterol (7KC: 50 μ M, 48 h) in the presence or absence of α -tocopherol (α -toco: 400 μ M), used as a positive control for cytoprotection, or with α -linolenic acid (ALA), eicosapentaenoic acid (EPA), docosahexaenoic acid (DHA), and oleic acid (OA) used at 25 μ M. Apoptosis was evaluated by caspase-3, -7, -9 activation (cleaved caspase), and PARP fragmentation. Autophagy was evaluated by conversion of LC3-I to LC3-II (increased LC3-II/LC3-I ratio). The EtOH value (0.5 %) correspond to the final EtOH concentration in the culture medium. β -actin was used as the loading control. Data shown are representative of three independent experiments. Significance of the differences between control (untreated cells), and vehicle (EtOH 0.5 %)-, ALA-, EPA-, DHA-, OA-, α -toco- or 7KC-treated cells; Mann-Whitney test: * $p < 0.05$ or less. Significance of the differences between 7KC-treated cells and (7KC + (ALA, EPA, DHA, OA or α -toco))-treated cells; Mann-Whitney test: # $p < 0.05$ or less. No difference was observed between control and vehicle-treated cells as well as between control, vehicle, α -toco, ALA, EPA and DHA.

absolute ethanol.

Quantification of cell viability by the fluorescein diacetate (FDA) assay

N2a cells viability was assessed using a lipophilic fluorochrome, fluorescein diacetate (FDA) (Sigma-Aldrich) (Ghzaïel et al., 2023; Kamiloglu et al., 2020). In the presence of esterases of living cells, the non-fluorescent FDA is transformed into a green, fluorescent metabolite "fluorescein". At the end of the treatment, cells were incubated in the dark with FDA (15 µg/mL, 5 min, 37°C), washed twice with phosphate buffer saline (PBS 0.1 M, pH 7.4), and then lysed with 10 mM Tris-HCl solution containing 1 % sodium dodecyl sulfate (SDS). Fluorescence intensity of fluorescein was measured with excitation at 485 nm and emission at 528 nm using a microplate reader (Sunrise spectrophotometer, TECAN, Lyon, France) in order to quantify living cells. All assays were performed in at least four independent experiments and realized in triplicate. The results were expressed as % of control: (Fluorescence (assay) × 100)/Fluorescence (control).

Flow cytometric evaluation of plasma membrane permeability and cell death by staining with propidium iodide

Propidium iodide (PI) has two quaternary ammoniums, the second one being relatively hydrophilic. This implies that viable cells, which have intact plasma membranes, will not permit intracellular PI accumulation; a contrary, dead cells, with altered membranes, will permit intracellular PI accumulation and further DNA binding (Yeh et al., 1981). When excited by a blue light (488 nm), PI emits an orange / red fluorescence. The stock solution of PI was prepared in milliQ water at a concentration of 1 mg/mL. To determine the role of phosphoinositide 3-kinase (PI3-K) in the protective effects of fatty acids against 7KC-induced cell death, N2a cells were pretreated with LY-294002 (Cell Signaling Technology, Danvers, MA, USA) - a PI3-K inhibitor - at 20 µM for 1 h, and then treated with 7KC associated or not with fatty acids. Furthermore, to determine the role played by catalase and GPx in cell viability, inhibitors of these enzymes (catalase: 3-aminotriazole (3-AT, 2 mM) (Mu et al., 2021); GPx: mercaptosuccinic acid (MSA, 3 mM) (Quispe et al., 2018) were added 1 h before treating cells with 7KC associated or not with fatty acids or α-tocopherol. At the end of treatments, N2a cells (adherent and non-adherent cells) were stained with a PI solution at 1 µg / mL in 1X PBS for 5 min at 37 °C. The cells were immediately analyzed on a BD Accuri™ C6 flow cytometer (Becton-Dickinson) and the fluorescence of PI was selected on a 630 nm long pass filter. Ten thousand cells were acquired per sample, and the fluorescence was quantified on a logarithmic scale. Data were analyzed with FlowJo software (Tree Star Inc.). The percentage of dead cells corresponds to the percentage of PI positive cells. At least three independent experiments were realized.

Morphological characterization of apoptotic cells by nuclear staining with Hoechst 33342

Nuclear morphology can be assessed by staining with Hoechst 33342. If the staining pattern of the nuclei is uniform, the cells are considered as viable cells; if the nuclei are condensed and/or fragmented, the cells correspond to apoptotic cells (Lizard et al., 1995). After staining with Hoechst 33,342 (2 µg/mL), the nuclear morphology was examined in the presence or absence of LY-294002 (a PI3-K inhibitor used at 20 µM) associated or not with 7KC (50 µM) with or without fatty acids (ALA, EPA, DHA, or OA; 25 µM) or α-tocopherol (400 µM) using an Axioskop right microscope (Zeiss, Jena, Germany) under ultraviolet light. A total of 300 cells per sample were counted to determine the percentage of apoptotic cells.

Flow cytometric measurement of transmembrane mitochondrial potential with DiOC₆(3)

The cationic lipophilic dye 3, 3' - dihexyloxacarbocyanine iodide DiOC₆(3) is a green-fluorescent, cell-permeable lipophilic dye that is selective for mitochondria, and which is used to evaluate *trans*-membrane mitochondrial potential ($\Delta\Psi_m$). The higher the $\Delta\Psi_m$, the more DiOC₆(3) accumulates. Thus, mitochondria of living cells will be more fluorescent than mitochondria of dead and dying cells containing depolarized mitochondria characterized by a lower $\Delta\Psi_m$ indicated by a decrease in the green fluorescence of DiOC₆(3) collected through a 520 ± 10 nm band pass filter on a BD Accuri™ C6 flow cytometer (Becton-Dickinson) (Ghzaïel et al., 2022). In the present study, $\Delta\Psi_m$ was measured on cells that were treated for 48 h with or without 7KC (50 µM) in the presence or absence of fatty acids (ALA, EPA, DHA, or OA; 25 µM). In addition, to study the role of GSK3 in 7KC-induced toxicity, N2a cells were pre-incubated with a GSK3 inhibitor (SB216763, 15 µM; Cell Signaling Technology) for 2 h and then treated with 7KC (50 µM) associated or not with fatty acids (ALA, EPA, DHA, or OA; 25 µM). At the end of treatments, N2a cells were stained for 15 min at 37°C with DiOC₆(3) (Thermo Fisher Scientific) used at 40 nM. For each sample, 10,000 cells were acquired on a BD Accuri™ C6 flow cytometer (Becton-Dickinson), and data were analyzed with FlowJo software (Tree Star Inc.). At least three independent experiments were realized.

Flow cytometric measurement of reactive oxygen species with dihydroethidine

Reactive Oxygen Species (ROS) overproduction, including the intracellular superoxide anion ($O_2^{\bullet-}$), was detected by staining with dihydroethidine (DHE). DHE is not a fluorescent probe; it diffuses through cell membranes, and when ROS are present, it is oxidized to hydroethidium (HE) which is a fluorescent compound with an orange/red fluorescence (λ Ex max = 488 nm; λ Em max = 575 nm) (Ghzaïel et al., 2022). HE is an intercalator of DNA. The stock solution of DHE (Thermo Fisher Scientific, Brumath, France) was prepared in DMSO at a concentration of 10 mM, and was subsequently used on the cells at a final concentration of 2 µM. To evaluate ROS production, N2a cells, previously cultured for 24 h, were incubated for 48 h with or without 7KC (50 µM) in the presence or absence of fatty acids (ALA, EPA, DHA, or OA; 25 µM) or α-tocopherol (400 µM). At the end of the treatment, N2a cells were trypsinized, washed and suspended in 1 mL of 1X PBS containing DHE (2 µM). After 15 min of incubation at 37 °C, the analysis of stained cells was carried out by flow cytometry on a BD Accuri™ C6 flow cytometer (Becton-Dickinson, Franklin Lakes, NJ, USA). To determine whether 7KC-induced ROS overproduction results from stimulation of NAD(P)H oxidase activity, diphenyleneiodonium chloride (DPI; ref: 2926, Sigma-Aldrich) - a selective NAD(P)H oxidase inhibitor - was added at 10 µM, 1 h before 7KC (Pedruzzi et al., 2004). In addition, to clarify the role played by catalase and glutathione peroxidase (GPx) in the overproduction of ROS, inhibitors of these enzymes (catalase: 3-aminotriazole (3-AT, 2 mM; ref: A8056, Sigma-Aldrich); GPx: mercaptosuccinic acid (MSA, 3 mM; ref: M6182, Sigma-Aldrich)) were added 1 h before treating the cells with 7KC associated or not with fatty acids or α-tocopherol. The fluorescence of HE was collected through a 580 nm band pass filter. Ten thousand cells were acquired per sample, and the fluorescence was quantified on a logarithmic scale. The data were analyzed with FlowJo software v10.6.2 (Tree Star Inc., Ashland, OR, USA). The percentage of ROS producing cells corresponds to the percentage of DHE positive cells. At least three independent experiments were realized.

Flow cytometric measurement of mitochondrial reactive oxygen species production with MitoSOX-Red

For the detection of ROS, especially $O_2^{\bullet-}$ in the mitochondria, the

MitoSOX-Red mitochondrial superoxide indicator was used. In the mitochondria, this probe is oxidized by ROS and emits an orange / red fluorescence (λ Ex max = 510 nm; λ Em max = 580 nm). The oxidation product becomes highly fluorescent upon binding to nucleic acids (Ksila et al., 2023). A stock solution of MitoSOX-Red (Thermo Fisher Scientific) was initially prepared at 5 mM in PBS. Briefly, after treating N2a cells for 48 h with or without 7KC (50 μ M) in the presence or absence of fatty acids (25 μ M) or α -tocopherol (400 μ M), adherent and non-adherent cells were incubated with 5 μ M MitoSOX-Red in PBS (15 min, 37 °C). Flow cytometric analyses were immediately performed. The fluorescent signals were detected through a 580 \pm 20 nm band pass filter using a BD Accuri™ C6 flow cytometer (Becton-Dickinson). For each sample, 10,000 cells were acquired. Data were analyzed with FlowJo software (Tree Star Inc). At least three independent experiments were realized.

Evaluation of lipid peroxidation by flow cytometric quantification of 4-hydroxynonenal

4-hydroxynonenal (4-HNE) is a by-product of lipid peroxidation; it is widely accepted as a stable marker for oxidative stress (Milkovic et al., 2023). To identify and quantify 4-HNE, and 4-HNE adducts, we used flow cytometry by using the following protocol. At the end of the treatments, cells were collected by trypsinization, fixed in 2 % paraformaldehyde diluted in PBS, incubated with blocking buffer (PBS, 0.05 % saponin, 10 % fetal bovine serum), washed in PBS, and incubated with a rabbit polyclonal antibody raised against 4-HNE (Abcam, Paris, France) diluted in blocking buffer (2 μ g/mL; 1 h at room temperature (RT)). After washing with PBS, cells were incubated for 1 h at RT with a 488-Alexa goat anti-rabbit polyclonal antibody (Life Science Technologies) diluted at 1/300 in blocking buffer. After a PBS wash, cells were resuspended in PBS and analyzed by flow cytometry on a BD Accuri™ C6 flow cytometer. For each sample, 10,000 cells were acquired, and the data were analyzed with FlowJo software (Tree Star Inc).

Flow cytometric quantification of the level of the peroxisomal ABCD3 transporter: Evaluation of the peroxisomal mass

To evaluate changes in the peroxisomal mass, an indirect immunofluorescence method was used with an antibody raised against the peroxisomal transporter (ATP-binding cassette sub-family D member 3, ABCD3) (Debbabi et al., 2017). After trypsinization, and washing in PBS, adherent and non-adherent cells were fixed in 2 % (w/v) paraformaldehyde (Sigma-Aldrich) diluted in PBS (15 min, RT). After washing in PBS, the cells were incubated in PFS buffer (PBS / 5 % FBS / 0.05 % saponin (Sigma-Aldrich)) (30 min, RT). Furthermore, the cells were washed with PBS and incubated (1 h, RT) with a rabbit polyclonal antibody raised against ABCD3 (ref: #11523651, Thermo Fisher Scientific) diluted (1/500) in PFS buffer. After washing with PBS, cells were further incubated in the dark with a goat anti-rabbit secondary antibody coupled with Alexa 488 (Santa-Cruz Biotechnology, Santa Cruz, CA, USA) diluted (1/500) in PFS buffer (30 min, RT). After washing, the cells were resuspended in PBS and analyzed by flow cytometry on a BD Accuri™ C6 flow cytometer (Becton-Dickinson). 10,000 cells were analyzed, and the green fluorescence was collected through a 520 \pm 20 nm bandpass filter. Absolute and conjugated controls (cells without antibodies, and without primary antibody, respectively) were realized. Data were analyzed with FlowJo software (Tree Star Inc.).

Transmission electron microscopy of peroxisomes and mitochondria

Transmission electron microscopy was used to simultaneously visualize peroxisomes, and mitochondria in N2a cells cultured for 48 h in the absence or in the presence of 7KC (50 μ M) without or with fatty acids (ALA, EPA, DHA, or OA; 25 μ M) or α -tocopherol (400 μ M). The sample preparation technique used is specifically adapted to allow the detection of peroxisomes. Cells were fixed for 1 h at 4°C in 2.5 % (w/v)

glutaraldehyde diluted in a cacodylate buffer (0.1 M, pH 7.4), washed twice in cacodylate buffer, incubated in the dark for 1 h at 21 °C in Tris-HCl (0.05 M, pH 9.0) containing diaminobenzidine (DAB: 2.5 mg/mL) and H₂O₂ (10 μ L/mL of a 3 % solution); washed in cacodylate buffer (0.1 M, pH 7.4) for 5 min at 21 °C; post-fixed in 1 % (w/v) osmium tetroxide diluted in cacodylate sodium (0.1 M, pH 7.4) for 1 h at 21 °C in the dark; and rinsed in cacodylate buffer (0.1 M, pH 7.4). The preparations were dehydrated in graded ethanol solutions and then embedded in Epon. Ultrathin sections were cut with an ultramicrotome, contrasted with uranyl acetate and lead citrate, and examined using an HT7800 electron microscope (Hitachi, Tokyo, Japan).

Quantification of catalase activity

Catalase is a peroxisomal enzyme that degrades hydrogen peroxide (H₂O₂) into water and molecular oxygen (2 H₂O₂ \rightarrow 2 H₂O + O₂). Catalase activity was evaluated following a photometric measurement of the H₂O₂ decomposition by catalase contained in the cell extract at 240 nm (Ghzaiel et al., 2023). A reaction mixture of H₂O₂ solution (30 %) and Tris-HCl buffer (1 M, pH 7.4) was added to the cell extract, and the reaction was carried out for 2 min. One unit of the enzyme is defined as 1 μ mol of H₂O₂ consumed per minute, and the specific activity is reported as units per milligram of protein according to the following formula:

$$\text{Catalase specific activity} = \left(\frac{\Delta Abs_{240nm} \cdot \text{min}^{-1}}{43.2} \right) \times 10^6 \times (200/10) \times (1/[\text{protein}] \text{mg} \cdot \text{l}^{-1})$$

The absorbance at 240 nm was read on a Tecan Infinite M 200 Pro (Tecan, Männedorf, Switzerland). Protein content was determined with the Pierce TM BCA Protein Assay Kit (ref: 23227; Thermo Fisher Scientific). Data are presented as [(catalase activity in the assay) / (Catalase activity in control (untreated) cells)].

Quantification of superoxide dismutase activity

The Beauchamp and Fridovich's method was used to measure cellular superoxide dismutase (SOD) activity. The method is based on the ability of superoxide anion (O₂^{•-}) to reduce Nitro blue Tetrazolium (NBT) (Ghzaiel et al., 2023). SOD activity was measured with the following mixture prepared in phosphate buffer (50 mM, pH 7.8) containing Ethylenediaminetetraacetic acid (EDTA; 0.1 mM), riboflavin (2 μ M), L-methionine (13 mM) and NBT (75 μ M) which gives a bluish color; in the presence of SOD, present in the cell lysate, the oxidation of NBT is lower and the blue coloration decreases. Exposure to the light of the mixture to white was carried out for 20 min. SOD activity was measured at 560 nm on a Tecan Infinite M 200 Pro (Tecan). SOD units / mg of protein is expressed as:

$Y / 50$ with $Y = [(ODB-ODA) \times 100 \times 20 \times d] / [ODB \times X]$; ODB: Optical Density Blank; ODA: Optical Density Assay; X: quantity of protein in the sample (mg/mL); 20 (50 μ L of cell lysate); d: dilution factor. The protein content was determined with the Pierce TM BCA Protein Assay Kit (Thermo Fisher Scientific). Data are presented as [(SOD activity in the assay) / (SOD activity in control (untreated) cells)].

Quantification of glutathione peroxidase activity

The method of Flohé and Günzler was used to determine the glutathione peroxidase (GPx) activity. GPx degrades hydrogen peroxide (H₂O₂) into water and GSSG (2GSH + H₂O₂ \rightarrow 2 H₂O + GSSG) (Ghzaiel et al., 2023). Cell lysates were incubated with 0.1 mM reduced glutathione (GSH, 0.1 mM) in TPO₄ (50 mM, pH 7.8). The reaction was initiated by adding H₂O₂ (1.3 \times 10⁻³ M) and stopped by incubating the mixture with trichloroacetic acid (1 % TCA) for 30 min at 4 °C and then centrifuged (1,000 \times g, 10 min). Further, the supernatant is incubated with DTNB / Na₂HPO₄·12H₂O for 10 min and the absorbance is read by

spectrophotometry at 412 nm on a Tecan Infinite M 200 Pro (Tecan). The activity of GPx is expressed in μmol of GSH consummate / min / mg of protein. The protein content was determined with the Pierce TM BCA Protein Assay Kit (Thermo Fisher Scientific). Data are presented as [(GPx activity in the assay) / (GPx activity in control (untreated) cells)].

Protein analysis: Polyacrylamide gel electrophoresis and western blotting

Protein analysis by electrophoresis was performed on polyacrylamide gel and Western blot. After 48 h of treatment, adherent and non-adherent cells were collected, washed in PBS and lysed for 30 min on ice in RIPA buffer (10 mM Tris-HCl, pH 7.2, 150 mM NaCl, 0.5 % Nonidet NP40, 0.5 % Na deoxycholate, 0.1 % SDS, 2 mM EDTA and 50 mM NaF) containing a complete cocktail of protease inhibitors (Roche Diagnostics, Indianapolis, IN, USA) diluted to 1/25. Cell debris were removed by centrifugation (20 min, 20,000 g) and the supernatant was isolated. Protein concentration was determined using bicinchoninic acid reagent (Sigma-Aldrich). Fifty micrograms of protein were used along with loading buffer (125 mM Tris-HCl, pH 6.8, 10 % β -mercaptoethanol, 4.6 % SDS, 20 % glycerol, and 0.003 % bromophenol blue). The proteins were separated on a 14 % or 8 % SDS-PAGE gel, and a transfer onto a nitrocellulose membrane was then carried out (Bio-Rad, Marne La Coquette, France). The membranes were further incubated for 1 h with 5 % powdered milk in PBST (PBS, 0.1 % Tween 20, pH 7.2) to block non-specific binding sites. The membrane was then brought into contact overnight (4 °C) with the primary antibody diluted in 5 % PBST milk. Various primary antibodies were used to demonstrate the induction of apoptosis and/or autophagy: an antibody against caspase-3 to detect endogenous levels of full-length caspase-3 (35 kDa) and cleaved caspase-3 (17 kDa) (rabbit polyclonal antibody; Cell Signaling, ref: #9662); an antibody directed against caspase-7 to detect endogenous levels of full-length caspase-7 (35 kDa) and cleaved caspase-7 (20 kDa) (rabbit polyclonal antibody; Cell Signaling, ref: 9492), an antibody directed against caspase-9 to detect endogenous levels of full-length caspase-9 (49 kDa) and cleaved caspase-9 (37 kDa) (mouse monoclonal antibody; Cell Signaling, ref: 9508), an antibody against PARP (poly-ADP-ribose polymerase) to detect endogenous level of full-length PARP (110 kDa) and the cleaved 89 kDa fragment of PARP (rabbit mAb; Cell Signaling, ref: 9532), and an antibody against LC3 for the detection of LC3-I (18 kDa) and LC3-II (16 kDa) (rabbit polyclonal antibody; Sigma-Aldrich, ref: L8918); these antibodies were used at a final dilution of 1/1000. For the analysis of oxidative stress, the following antibodies were used: Nrf2 (rabbit polyclonal antibody, CliniSciences, Nanterre, France; ref: C0279), Nrf2 (phospho Ser 40) (rabbit polyclonal antibody, CliniSciences / GeneTex, Irvine, CA, USA; ref: GTX02873), GPx1 (rabbit polyclonal antibody, CliniSciences / GeneTex; ref: GTX116040-S), SOD1 (rabbit polyclonal antibody, CliniSciences / GeneTex; ref: GTX100554-S) and catalase (goat polyclonal antibody, R&D systems, Abingdon, UK; ref: AF3398). The rabbit polyclonal antibodies were used at a final dilution of 1/1000. The polyclonal goat antibody raised against catalase was used at a final dilution of 1/400. For the study of the PI3-K/PDK-1/Akt signaling pathway, the following antibodies were used at a 1/1000 dilution: polyclonal anti-Akt antibody (rabbit polyclonal antibody, Cell Signaling, ref: 9272), polyclonal anti-phospho-Akt Thr 308 antibody (rabbit mAb, Cell Signaling, ref: 4056), anti-PDK1 monoclonal antibody (mouse monoclonal antibody, Santa-Cruz, ref: sc-515944) and anti-PDK-1 phospho Tyr 373/376 polyclonal antibody (rabbit polyclonal antibody, Cell Signaling, ref: 3065). For the GSK3/Mcl1 signaling pathway, the following antibodies were used: anti-GSK3 α/β (mouse monoclonal antibody, Santa Cruz Biotechnology, ref: sc-7291), anti-phospho-GSK3 α/β (ser21/9) (rabbit polyclonal antibody, Cell Signaling, ref: 9331), and anti-Mcl-1 (rabbit mAb, Abcam, ref: Ab32087). An antibody directed against β -actin (mouse monoclonal antibody, Sigma-Aldrich, ref: A2228;) was used at a final concentration of 1/10,000 for standardization. Three 10-minutes washes with PBST were performed, and the membranes were incubated for 1 h at RT with horseradish

peroxidase-conjugated goat anti-rabbit secondary antibody (Cell Signaling, ref: 7074) or anti-mouse antibody (Santa Cruz Biotechnology, ref: sc-2005) diluted 1/5,000 in 1 % PBST milk powder (PBS, 0.1 % Tween 20, pH 7.2). The membranes were then washed with PBST and the presence of antibodies was revealed using an enhanced chemiluminescence detection kit (Supersignal West Femto Maximum Sensitivity Substrate, Thermo Fisher Scientific) and the Chemidoc XRS + apparatus (Bio-Rad). The protein level was calculated with the Image Lab software (Bio-Rad).

Real time quantitative-PCR (RT-qPCR) analysis

The RNeasy Mini Kit (Qiagen, Courtaboeuf, France) made it possible to extract and purify the total mRNAs obtained from N2a cells after 48 h of treatment with fatty acids (ALA, EPA, DHA, or OA; 25 μM) without or with 7KC (50 μM). Total mRNA concentration was measured with TrayCell (Hellma, Paris, France) by spectrophotometry (UV-1800 spectrophotometer, Shimadzu, Kyoto, Japan) at an absorbance of 260 nm and calculated with UV Probe (Shimadzu software, Shimadzu France, Marne la Vallée, France). The absorbance ratio at 260 nm and 280 nm was used to control the purity of nucleic acids (ratios of 1.8 to 2.2 were considered satisfactory). Once the concentrations were calculated, 1 μg of total mRNA from each sample was converted to single-stranded cDNA using the iScript cDNA Synthesis Kit (BioRad, Marne la Coquette, France) using the following procedure: 5 min at 25 °C, 20 min at 46 °C, and 5 min at 95 °C. Amplification of cDNA was performed in the presence of Takyon TM Rox SYBR Master Mix dTTP Blue (Eurogentec, Liège, Belgium), and 300 nM mouse forward and reverse primers (Eurogentec).

The primer sequences used were as follows:

- Nrf2: Forward 5'-CAGCATGTTACGTGATGAGG-3' and Reverse 5'-GCTCAGAAAAGGCTCCATCC-3'
- NQO1: Forwards 5'-AGGATGGGAGGTACTCGAATC-3' and Reverse 5'-AGGCGTCCTTCCTTATATGCTA-3'
- HMOX-1: Forward 5'-CACAGCACTATGTAAGCGTCT-3' and Reverse 5'-GTAGCGGGTATATGCGTGGG-3'
- GPx1: Forward 5'-CCACCGTGTATGCCTTCTCC-3' and Reverse 5'-AGAGAGACGCGACATTCTCAAT-3'
- Sod1: Forward 5'-AACCAGTTGTGTTGTCAGGAC-3' and Reverse 5'-CCACCATGTTTCTTAGAGTGAGG-3'
- Catalase: Forward 5'-CTCAGGACGATGAGGTTCTGCT- 3'and Reverse 5'-TGGCGAGACAA-TCCATCACTG-3'

Quantitative real-time polymerase chain reaction (PCR) products of reverse-transcribed cDNA samples were detected by StepOne Plus (Life Technologies/Thermo Fischer Scientific). The thermal cycler was set up as follows: activation of DNA polymerase at 95 °C for 10 min, followed by 40 cycles of amplification at 95 °C for 15 secondes, 60 °C for 30 secondes and 72 °C for 30 secondes, with a check for the absence of non-specific products via analysis of the melting curve. Gene expression (mRNA level) was quantified using cycle-to-threshold (Ct) values and normalized by reference gene 36B4 (Forward 5'-GCGACCTGGAAGTCAACTA-3' and Reverse 5'-ATCTGCTTGGAGCCACAT-3'). Specific amplification efficiencies were calculated with StepOne software (Life Technologies/Thermo Fischer Scientific). The quantitative expression (mRNA level) of the studied genes was determined as a control induction

factor.

Statistical analysis

Statistical analyses were performed using XLSTAT software (Microsoft). Data were expressed as mean \pm standard deviation (SD); data were considered statistically different (Mann–Whitney test) at a p -value of 0.05 or less.

Results

Effects of α -linolenic acid, eicosapentaenoic acid, docosahexaenoic acid, oleic acid and α -tocopherol on 7-ketocholesterol-induced cell death: evaluation by western blotting of apoptotic and autophagic criteria

On N2a cells, our data show that 7KC (50 μ M, 48 h) is an inducer of apoptosis and autophagy associated with oxidative stress. This set of processes has been defined as oxiaoptophagy (Nury et al., 2020). In the N2a neuroblastoma line, 7KC was used at 50 μ M for 48 h (conditions defined above, (Yammine et al., 2020)). In these conditions, 7KC induces apoptosis characterized by cleavage of caspase-3 (presence of a

cleaved fragment at 17 kDa), caspase-9 (presence of a cleaved fragment at 37 kDa) and caspase-7 (presence of a cleaved fragment at 20 kDa) (Fig. 1). This activation of caspases is supported by a cleavage of the PARP protein (presence of a cleaved fragment at 89 kDa) (Fig. 1). Western blotting experiments also reveal the presence of a conversion of LC3-I (18 kDa) to LC3-II (16 kDa) assessed by the LC3-II/LC3-I ratio which highlight the induction of an autophagic process. When N2a cells were simultaneously treated with 7KC (50 μ M) combined with ALA, EPA, DHA, OA (25 μ M) or α -tocopherol (400 μ M), used as a reference cytoprotective molecule, apoptosis was counteracted and autophagy was normalized: thus, levels of cleaved caspase-3,7,9, fragmented PARP, and LC3-II were strongly reduced compared with 7KC alone. In addition, the impact of 7KC on the peroxisome and mitochondria was also studied. In 7KC-treated cells, the oxiaoptophagic process induces a decrease of ABCD3 level, measured by flow cytometry, supporting a decrease of peroxisomal mass (Fig. 2A) associated with an increase of morphologically abnormal peroxisomes slightly stained with diamino benzidine (DAB) (Fig. 2B). Similarly, under treatment with 7KC, morphologically abnormal mitochondria, with a decrease in mitochondrial cristae, were observed (Fig. 2B). These different changes were strongly attenuated in the presence of ALA, EPA, DHA, OA and α -tocopherol when these

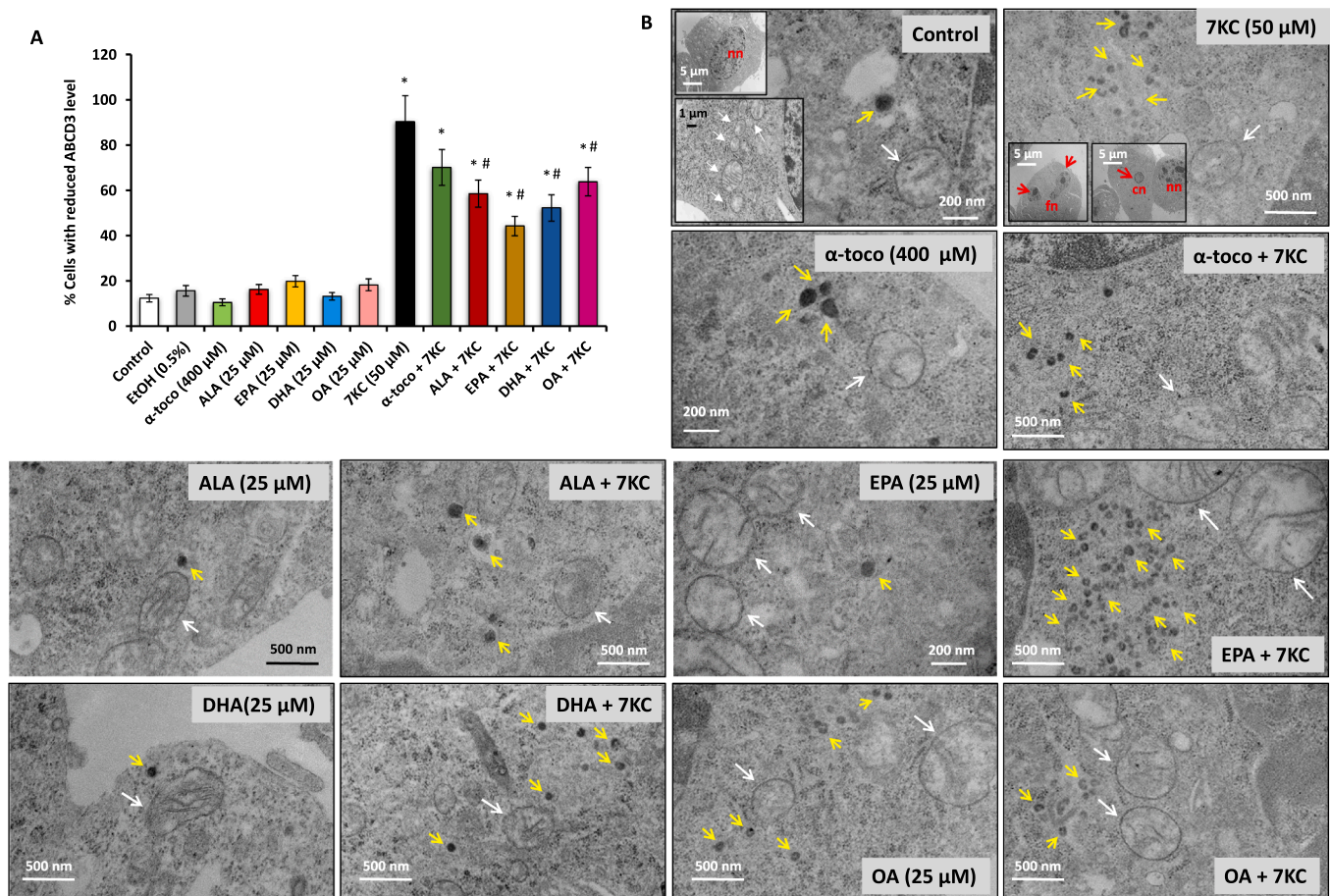


Fig. 2. Effects of α -linolenic acid, eicosapentaenoic acid, docosahexaenoic acid, oleic acid, and α -tocopherol on 7-ketocholesterol-induced mitochondrial and peroxisomal changes. N2a cells previously cultured for 24 h were further cultured for 48 h with or without 7-ketocholesterol (7KC, 50 μ M) in the presence or absence of α -linolenic acid (ALA), eicosapentaenoic acid (EPA), docosahexaenoic acid (DHA), and oleic acid (OA) used at 25 μ M or with α -tocopherol (α -toco: 400 μ M), used as a positive control for cytoprotection. **A.** Flow cytometric analysis of ABCD3 peroxisomal mass biomarker. **B.** Transmission electron microscopy showing mitochondria and peroxisomes with white and yellow arrows, respectively. The number of peroxisomes, materialized by a reduced ABCD3 level (percentage of cells with decreased abcd3 fluorescence) or detected by electron microscopy, is similar between control and fatty acids. In untreated N2a cells or fatty acid-treated cells, isolated peroxisomes were rarely detected in the cytoplasm. In 7-ketocholesterol-treated cells, more peroxisomes were detected in the cytoplasm and were present in clusters. Treatment with fatty acids reduced the presence of peroxisomes in the cytoplasm during treatment with 7KC. Significance of the differences between control (untreated cells), and vehicle (EtOH 0.5 %)-, ALA-, EPA-, DHA-, OA-, α -toco- or 7KC-treated cells; Mann–Whitney test: * $p < 0.05$ or less. Significance of the differences between 7KC-treated cells and (7KC + (ALA, EPA, DHA, OA or α -toco))-treated cells; Mann–Whitney test: # $p < 0.05$ or less. (For interpretation of the references to color in this figure legend, the reader is referred to the web version of this article.)

compounds were associated with 7KC (Fig. 2B), and the effect of fatty acids was often stronger than that of α -tocopherol. In fact, for the study of peroxisomes, fatty acids can be classified as follows, from the one with the greatest effect to the one with the least: EPA > DHA > ALA > OA > α -tocopherol. Comparatively to untreated cells (control) and vehicle (EtOH 0.5 %)-treated cells, no effects of ALA, EPA, DHA, OA and

α -tocopherol were found on ABCD3 level as well as on peroxisomal and mitochondrial morphology (Fig. 2A-B).

Altogether, our data show that ALA, EPA, DHA, and OA strongly attenuate 7KC-induced oxyapoptophagy, and have cytoprotective activities. In addition, ALA, EPA, DHA, OA, and α -tocopherol also oppose 7KC-induced peroxisomal and mitochondrial changes. It was therefore

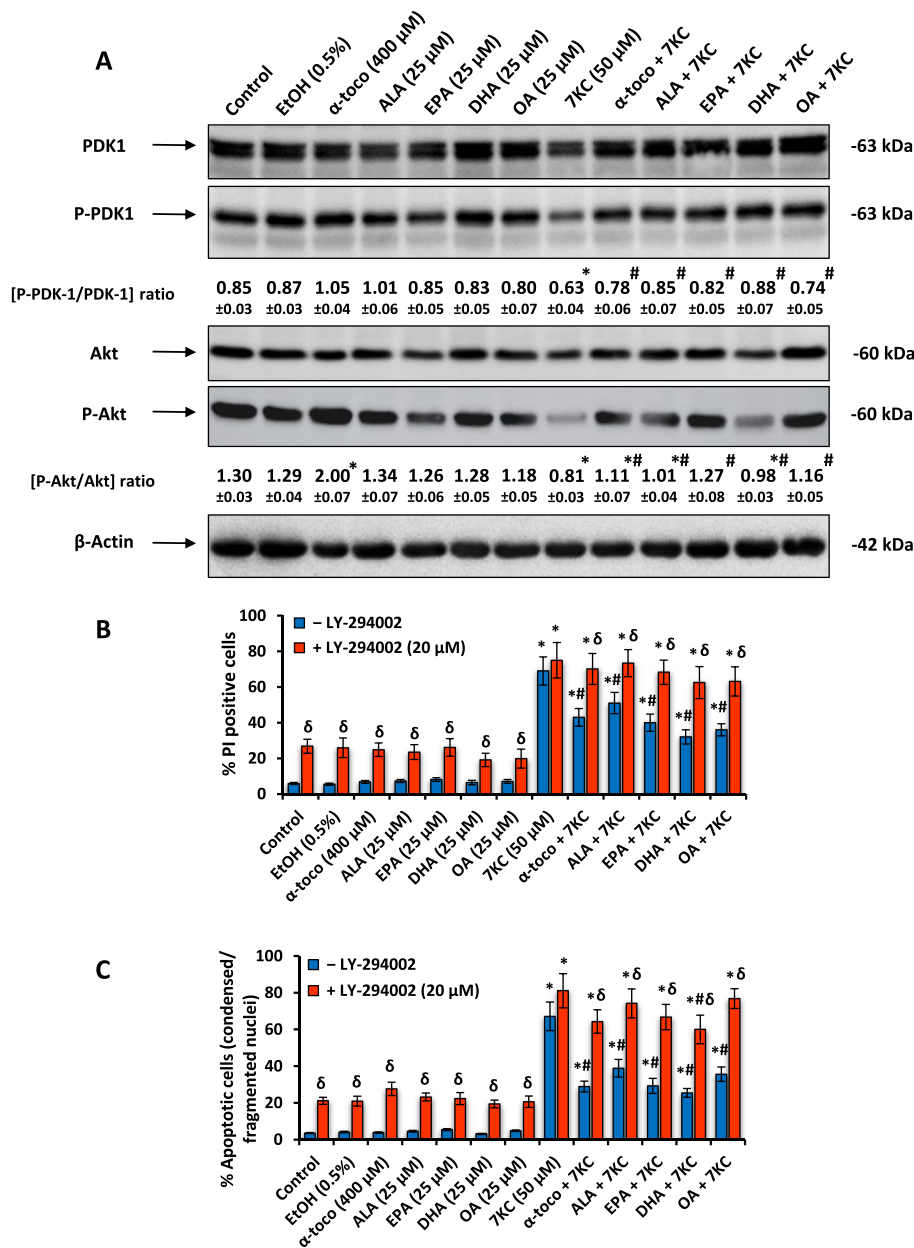


Fig. 3. Effects of α -linolenic acid, eicosapentaenoic acid, docosahexaenoic acid, oleic acid, and α -tocopherol on PI3-K / Akt signaling pathway in 7-ketocholesterol-treated cells. N2a cells previously cultured for 24 h were further cultured for 48 h with or without 7-ketocholesterol (7KC, 50 μ M) in the presence or absence of α -linolenic acid (ALA), eicosapentaenoic acid (EPA), docosahexaenoic acid (DHA), oleic acid (OA) used at 25 μ M or with α -tocopherol (α -toco: 400 μ M), used as a positive control for cytoprotection. **A.** Representative western blots for analysis related to the PI3-K / Akt (PKB) signaling pathway are shown total PDK-1 (PDK-1) and phosphorylated PDK-1 (P-PDK-1), and total Akt (Akt) and phosphorylated Akt (P-Akt) are shown. β -actin was used as the loading control. The intensities of the bands for each set were individually determined and are presented as the ratio over β -actin signal. **B.** Plasma membrane permeability was measured by flow cytometry after staining with propidium iodide (PI) which enters dead cells only. The role played by the PI3-K / Akt signaling pathway on 7KC-induced cell death was evaluated in the presence of LY-294002 which is a PI3-kinase inhibitor. **C.** Apoptosis was evaluated by Hoechst 33,342 staining which permits the identification of apoptotic cells characterized by condensed and/or fragmented nuclei. The role played by the PI3-K / Akt signaling pathway on 7KC-induced cell apoptosis was also evaluated in the presence of LY-294002. Significance of the differences between control (untreated cells), and vehicle (EtOH 0.5 %)-, ALA-, EPA-, DHA-, OA-, α -toco- or 7KC-treated cells; Mann–Whitney test: * $p < 0.05$ or less. Significance of the differences between 7KC-treated cells and (7KC + (ALA, EPA, DHA, OA or α -toco))-treated cells; Mann–Whitney test: # $p < 0.05$ or less. Significance of the differences between cells not treated with LY-294002 and LY-294002-treated cells; Mann–Whitney test: $\delta p < 0.05$ or less.

important to determine which signaling pathways may be involved in 7KC-induced cell death.

Evaluation of the involvement of the pre-mitochondrial PI3-K / Akt signaling pathway in 7KC-induced cell death and of the effects of α -linolenic acid, eicosapentaenoic acid, docosahexaenoic acid, oleic acid and α -tocopherol

The phosphoinositide 3-kinase (PI3-K) / Akt (PKB) pathway is an important second messenger system involved in both apoptosis and autophagy (Martelli et al., 2006; Sandoval). It was therefore important to determine the role played by the PI3-K / PDK-1 / Akt signaling pathway in 7KC-induced cell death and to determine the effects of ω 3 and ω 9 fatty acids (ALA, EPA, DHA, OA) on the phosphorylation status of PDK-1 and Akt. When N2a cells were treated with 7KC (50 μ M, 48 h), lower levels of the phosphorylated forms of PDK-1 and Akt were found,

and these effects were reduced by ALA, EPA, DHA, OA, and α -tocopherol (Fig. 3A). Thus, in N2a cells treated with 7KC, the PI3-K / PDK-1 / Akt signaling pathway is inactivated. The phosphorylation of PDK1 and Akt was restored when N2a cells were simultaneously treated with 7KC in the presence of ALA, EPA, DHA, OA, and α -tocopherol (Fig. 3A). However, the ability of ALA, EPA, DHA, OA, and α -tocopherol to oppose 7KC-induced cell death (measured by staining with propidium iodide (PI) and by nuclei staining with Hoechst 33,342 allowing the identification of apoptotic cells) was inhibited when ω 3 and ω 9 fatty acids were combined with LY-294002, an inhibitor of phosphoinositide 3-kinase (PI3-K). This result demonstrates that ALA, EPA, DHA, OA, and α -tocopherol positively regulate the activity of PI3-K, which plays a key role in the cytoprotective effect and control of 7KC-induced apoptosis (Fig. 3B-C).

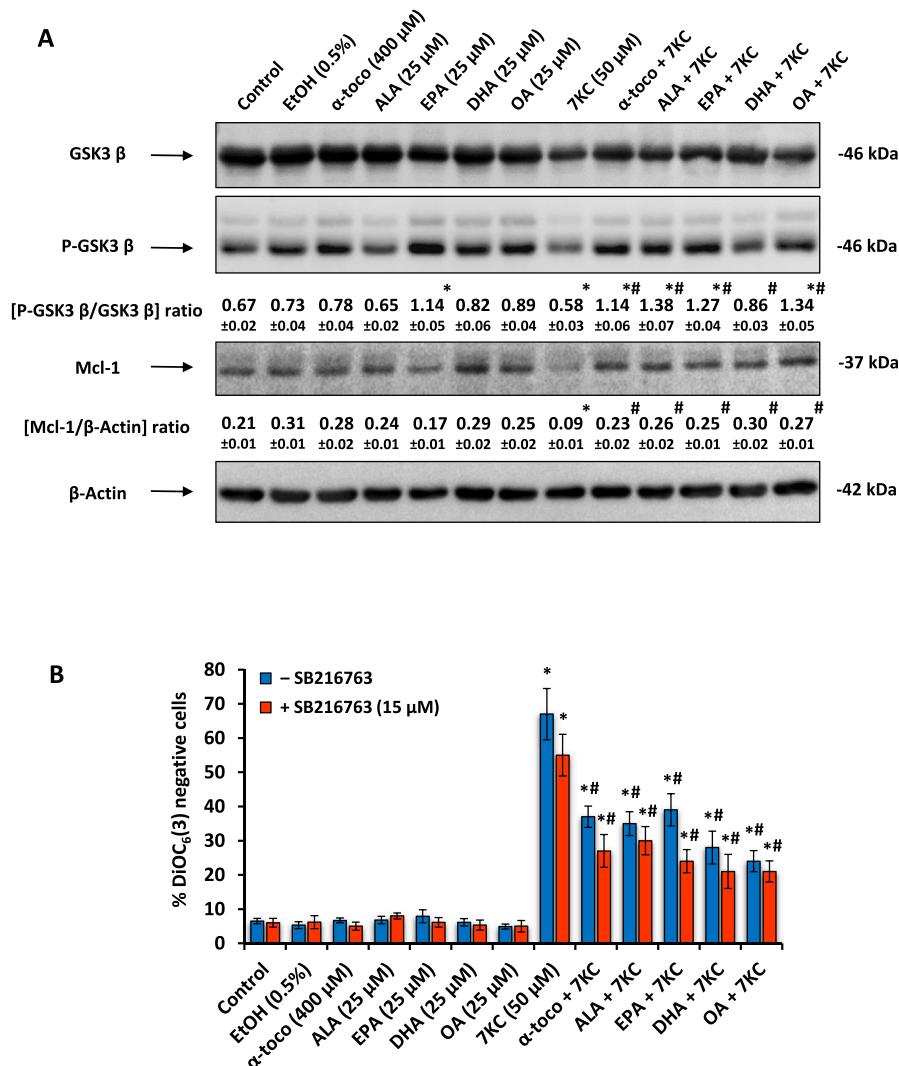


Fig. 4. Effects of α -linolenic acid, eicosapentaenoic acid, docosahexaenoic acid, oleic acid, and α -tocopherol on GSK-3/Mcl-1 signaling pathway in 7-ketocholesterol-treated cells. N2a cells previously cultured for 24 h were further cultured for 48 h with or without 7-ketocholesterol (7KC, 50 μ M) in the presence or absence of docosahexaenoic acid (DHA), eicosapentaenoic acid (EPA), α -linolenic acid (ALA), oleic acid (OA) used at 25 μ M or with α -tocopherol (α -toco: 400 μ M), used as a positive control for cytoprotection. **A.** Representative western blots were presented; they show protein level of total GSK3 β (GSK3 β), phosphorylated GSK3 β (P-GSK3 β) and total Mcl-1 (Mcl-1). The ratio of P-GSK3 β to GSK3 β was calculated to determine the proportion of P-GSK3 β protein and thus the activation of the pathway. β -actin was used as the loading control. The intensities of the bands for each set were individually determined and are presented as the ratio over β -actin signal. **B.** Transmembrane mitochondrial potential was measured by flow cytometry with the DiOC₆(3) fluorescent probe, and the percentage of cells with depolarized mitochondria (DiOC₆(3) negative cells) was determined. GSK3 inhibitor (SB216763) was used. Significance of the differences between control (untreated cells), and vehicle (EtOH 0.5 %)-, ALA-, EPA-, DHA-, OA-, α -toco- or 7KC-treated cells; Mann-Whitney test: * $p < 0.05$ or less. Significance of the differences between 7KC-treated cells and (7KC + (ALA, EPA, DHA, OA or α -toco))-treated cells; Mann-Whitney test: # $p < 0.05$ or less.

Evaluation of the involvement of the pre-mitochondrial GSK3 / Mcl-1 signaling pathway in 7KC-induced cell death and of the effects of α -linolenic acid, eicosapentaenoic acid, docosahexaenoic acid, oleic acid and α -tocopherol

The GSK3 / Mcl-1 pathway was studied for the following reasons: a) GSK3 β (glycogen Synthase Kinase 3 β) activity depends on Akt activity (Manning and Toker, 2017); b) mitochondrial transmembrane potential ($\Delta\Psi_m$) is in part under the control of Mcl-1 (Myeloid cell leukemia-1), a member of Bcl-2 family; this one is involved in the control of $\Delta\Psi_m$ (Letai, 2006; Wang et al., 2013). Furthermore, GSK3 β is known to contribute in neurodegeneration at different levels (Duda et al., 2018). Treatment of N2a cells with 7KC (50 μ M, 48 h) caused a decrease in GSK3 β phosphorylation, which is known to contribute to the degradation of Mcl-1 (Fig. 4A). With ALA, EPA, DHA, OA, and α -tocopherol, the decrease of phosphorylated GSK3 (P-GSK3) and of Mcl-1 was counteracted (Fig. 4A). These data demonstrate the involvement and the importance of the cascade of the pre-mitochondrial events (Akt / GSK3 / Mcl-1) in 7KC-induced cell death and show a link between cytoplasmic membrane alterations and mitochondrial depolarization leading to cell death. However, in the presence of SB216763, a inhibitor of GSK3, no significant effects were observed on $\Delta\Psi_m$ supporting a secondary role of the GSK3 in 7KC-induced mitochondrial depolarization and in the cytoprotective effects of ALA, EPA, DHA, OA, and α -tocopherol.

Effects of α -linolenic acid, eicosapentaenoic acid, docosahexaenoic acid, oleic acid and α -tocopherol on 7-ketocholesterol-induced oxidative stress

The changes observed at the level of the mitochondria and peroxisome, involved in the regulation of the RedOx equilibrium, led us to study the oxidative stress. Oxidative stress was assessed with MitoSOX-Red to detect mitochondrial production of superoxide anion ($O_2^{\bullet-}$) at the mitochondrial level, dihydroethidium (DHE) to assess the overproduction of ROS on whole cells, including superoxide anion ($O_2^{\bullet-}$), and hydroxyl radical (OH^{\bullet}). We also determined 4-HNE, a major end product of lipid peroxidation which strongly reacts with certain amino acid residues to form numerous 4-HNE adducts and favors protein carbonylation (Grimsrud et al., 2008). On N2a cells, 7KC (50 μ M, 48 h) induces oxidative stress with strong ROS overexpression: i) increased percentage of DHE-positive cells approximately 6-fold increase compared to untreated cells, ii) increased percentage of MitoSOX-positive cells approximately 6-fold increase compared to untreated cells, and iii) increased level of the lipid peroxidation biomarker 4-HNE, approximately 1.8-fold increase compared to untreated cells (Fig. 5). In the presence of ALA, EPA, DHA, OA, and α -tocopherol, 7KC-induced-oxidative stress was strongly attenuated: ROS overproduction at the mitochondrial level and on whole cells was significantly decreased as well as 4-HNE level (Fig. 5). Noteworthy, in the presence of a selective NAD(P)H oxidase inhibitor, diphenyleneiodonium (DPI), 7KC-induced ROS overproduction was inhibited at 40 % on whole cells (Fig. 5A). In the presence of DPI, the antioxidant activity of ALA, EPA and DHA on whole cells was also potentialized (Fig. 5A).

Evaluation of the effect of 7KC with or without α -linolenic acid, eicosapentaenoic acid, docosahexaenoic acid, oleic acid and α -tocopherol on Nrf2 phosphorylation and level, and on the expression Nrf2 and antioxidant target genes (NQO1, HMOX-1)

To prevent oxidative stress, cells have several defense mechanisms, one of them is the activation of the Nrf2 pathway, which regulates the expression of antioxidant genes, such as NAD(P)H: quinone oxidoreductase 1 (NQO1) and heme oxygenase 1 (HMOX-1) playing a crucial role in maintaining intracellular RedOx homeostasis (Song and Long, 2020). As 7KC, on N2a cells, is a strong inducer of ROS overproduction leading to lipid peroxidation and cell death, we determined the effects of 7KC and ω 3 and ω 9 fatty acids (ALA, EPA, DHA, OA) and α -tocopherol

on Nrf2 phosphorylation status by western blotting and on Nrf2 expression by RT-qPCR. As shown by western blot analysis and RT-qPCR, 7KC induced a decrease of Nrf2 phosphorylation (Fig. 6A) and expression (Fig. 6B). These effects are strongly and significantly attenuated by ALA, EPA, DHA, OA and α -tocopherol (Fig. 6A-B). In addition, these effects were associated with a decrease expression of NQO1 and HMOX-1, whose decrease was also counteracted by ALA, EPA, DHA, OA and α -tocopherol (Fig. 6B). In addition, to further investigate the involvement of PI3-K / Akt signaling pathway on the Nrf2 pathway, we used LY-294002, an inhibitor of phosphoinositide 3-kinases. Pretreatment with LY-294002 significantly inhibited the expression of Nrf2, NQO1, and HMOX-1 when 7KC was in the presence of ALA, EPA, DHA, OA and α -tocopherol. Altogether, these data demonstrate that 7KC neutralize the antioxidant Nrf2 signaling pathway, and that this later is restored in the presence of ALA, EPA, DHA, OA and α -tocopherol. They also indicate that the PI3-K / Akt pathway plays an important role in the activation of Nrf2 and the induction of NQO1 and HMOX-1 by ALA, EPA, DHA, OA, and α -tocopherol in N2a cells.

Role played by catalase, superoxide dismutase and glutathione peroxidase in 7-ketocholesterol-induced oxidative stress and effects of α -linolenic acid, eicosapentaenoic acid, docosahexaenoic acid, oleic acid and α -tocopherol

To better characterize oxidative stress and the sites of action of EPA, ALA, DHA, OA, and α -tocopherol we focused on the antioxidant enzymes catalase, glutathione peroxidase (GPx) and superoxide dismutase (SOD), especially GPx1 and SOD1. In presence of 7KC, the overproduction of ROS was associated with a significant decrease of GPx and SOD activities whereas catalase activity was enhanced (Fig. 7A). In the presence of EPA, ALA, DHA, OA, and α -tocopherol, GPx and SOD activities were significantly enhanced, catalase activity was significantly reduced (Fig. 7A). By Western blotting, in the presence of 7KC, decreased levels of GPx1 and SOD1 were observed as well as increased levels of catalase; these effects were counteracted in the presence of EPA, ALA, DHA, OA, and α -tocopherol (Fig. 7B). In addition, with 7KC, by RT-qPCR, a 50 % decrease expression of GPx1 was found by RT-qPCR, whereas Sod1 and catalase expression were enhanced (Fig. 8). 7KC-induced Sod1 decrease expression was counteracted by EPA, ALA, DHA, OA, and α -tocopherol and these cytoprotective effects were inhibited in the presence of LY-294002, an inhibitor of PI3-K (Fig. 8). 7KC-induced increase of Sod1 and catalase was significantly attenuated by EPA, ALA, DHA, OA, and α -tocopherol, and these effects were slightly more pronounced in the presence of LY-294002 (Fig. 8). In addition, the roles of catalase and GPx in ROS overproduction (evaluated by staining with DHE) and cell viability (evaluated by staining with PI), was determined with the use of enzymatic inhibitors: 3-aminotriazole (3-AT) for catalase; mercaptosuccinic acid (MSA) for GPx. 3-AT and MSA were used when N2a cells were treated with 7KC with and without ALA, EPA, DHA, OA and α -tocopherol. The results obtained showed a more important role of GPx than catalase in cytoprotection (Fig. 9). Thus, the data obtained show for the first time that restoration of GPx activity by ALA, EPA, DHA, OA and α -tocopherol is essential for the cytoprotective effect towards 7KC-induced ROS overproduction and cell death.

Discussion

Oxysterols are derived either from autoxidation or enzymatic oxidation of cholesterol, or both (Mutemberezi et al., 2016). Cholesterol autoxidation, associated with an excessive production of ROS is a common feature of several pathologies, especially age-related diseases including neurodegenerative diseases (Poli et al., 2013). Once produced or brought by a diet rich in processed foods, the major oxysterol formed by autoxidation (7KC) can in turn induce oxidative stress and cell death associated with apoptotic and autophagic criteria (Anderson et al., 2020). This type of cell death, which is defined as oxiapoptophagy (Nury et al., 2020), may be accompanied by inflammation. However, less

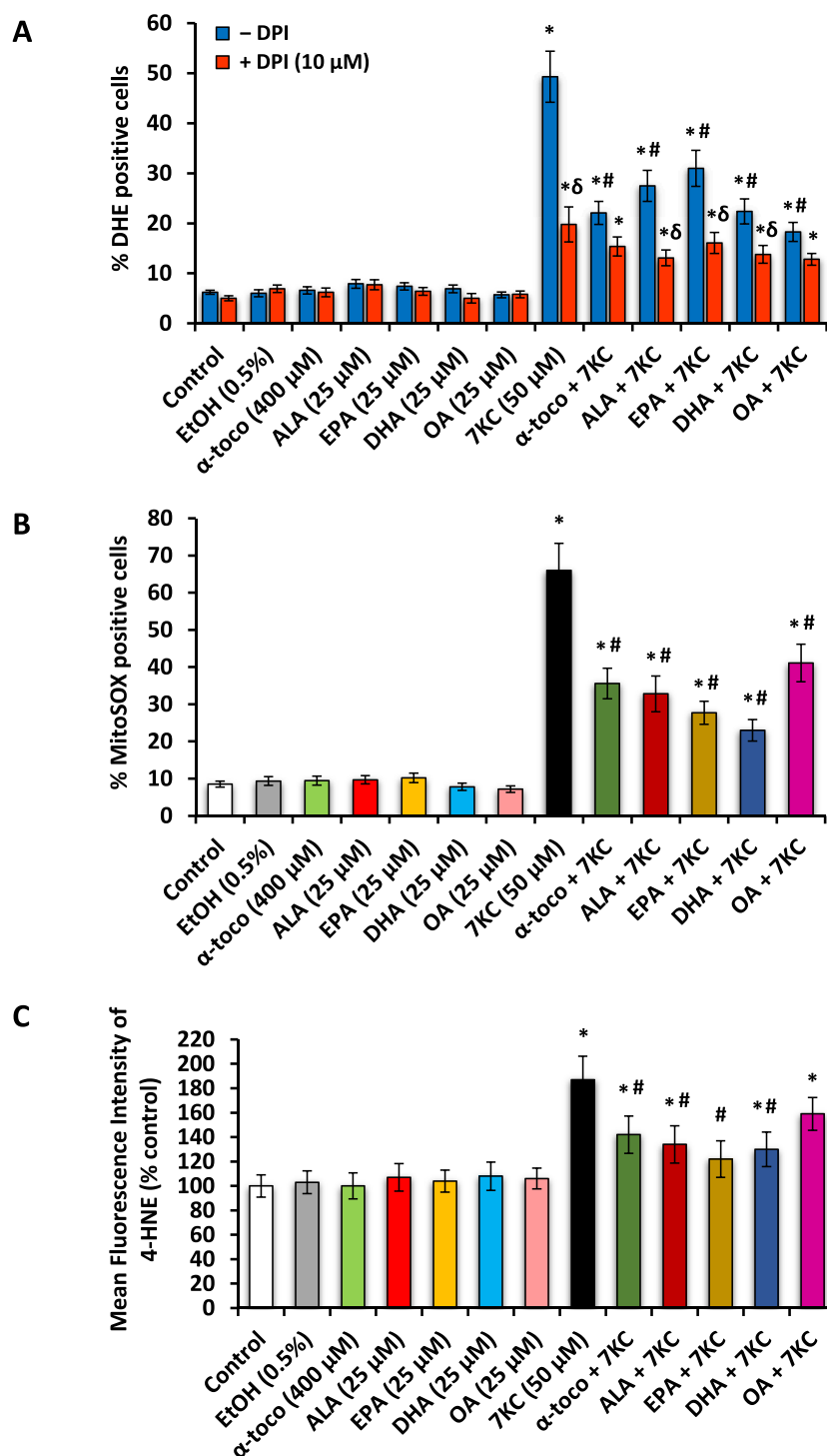


Fig. 5. Effect of α -linolenic acid, eicosapentaenoic acid, docosahexaenoic acid, oleic acid and α -tocopherol on 7-ketocholesterol-induced reactive oxygen species (ROS) overproduction. N2a cells previously cultured for 24 h were further cultured for 48 h with or without 7-ketocholesterol (7KC, 50 μ M) in the presence or absence of α -linolenic acid (ALA), eicosapentaenoic acid (EPA), docosahexaenoic acid (DHA), oleic acid (OA) used at 25 μ M or with α -tocopherol (α -toco: 400 μ M), used as a positive control for cytoprotection. ROS overproduction was measured by flow cytometry on whole cells after staining with dihydroethidine (DHE) (A), and at the mitochondrial level with MitoSox-Red (B). The incidence of ROS overproduction on lipid peroxidation was measured with 4-hydroxynonenal (4-HNE) (C). Diphenyleioidonium (DPI), a NAD(P)H inhibitor, was used to evaluate the implication of NAD(P)H in 7KC-induced ROS overproduction. Significance of the differences between control (untreated cells), and vehicle (EtOH 0.5 %), ALA-, EPA-, DHA-, OA-, α -toco- or 7KC-treated cells; Mann-Whitney test: * $p < 0.05$ or less. Significance of the differences between 7KC-treated cells and (7KC + (ALA, EPA, DHA, OA or α -toco))-treated cells; Mann-Whitney test: # $p < 0.05$ or less. Significance of the differences between cells not treated with DPI and DPI-treated cells; Mann-Whitney test: $\delta p < 0.05$ or less. (For interpretation of the references to color in this figure legend, the reader is referred to the web version of this article.)

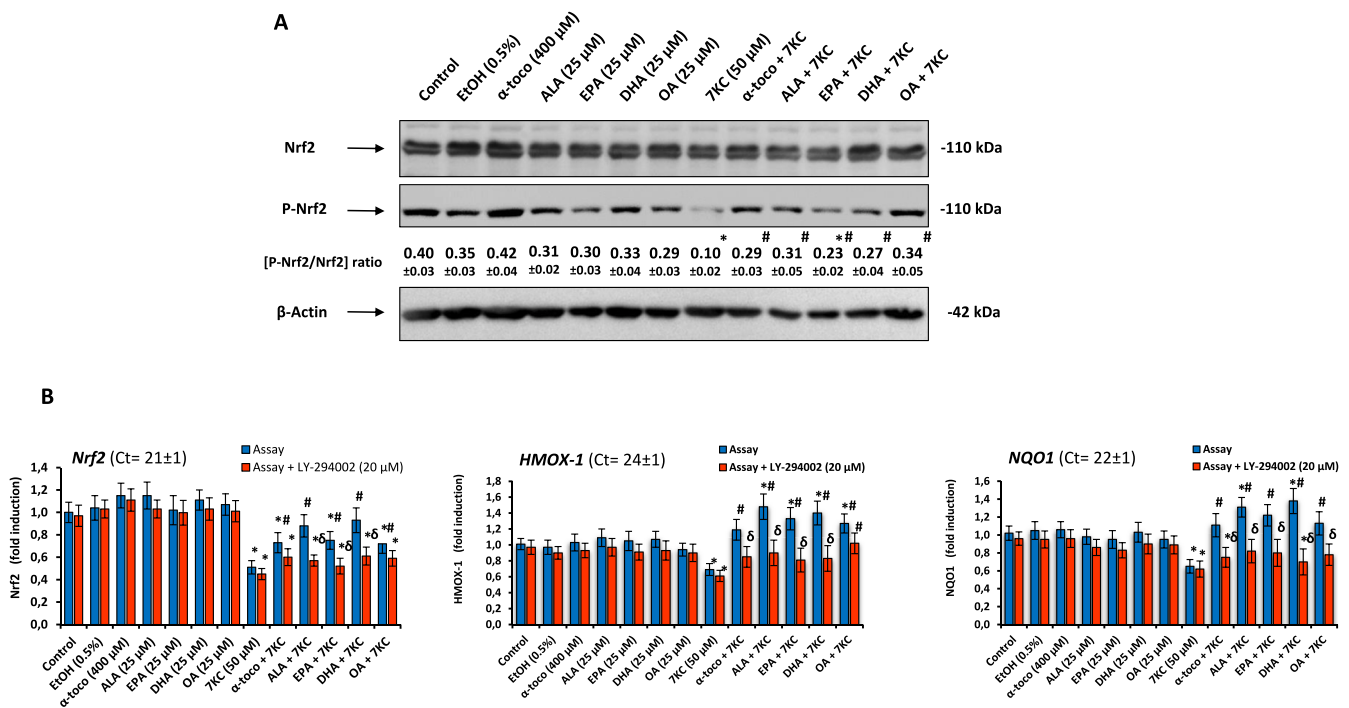


Fig. 6. Effects of 7-ketocholesterol with or without α -linolenic acid, eicosapentaenoic acid, docosahexaenoic acid, oleic acid, and α -tocopherol on the Nrf2 pathway. N2a cells previously cultured for 24 h were further cultured for 48 h with or without 7-ketocholesterol (7KC, 50 μ M) in the presence or absence of α -linolenic acid (ALA), eicosapentaenoic acid (EPA), docosahexaenoic acid (DHA), and oleic acid (OA) used at 25 μ M or with α -tocopherol (α -toco: 400 μ M), used as a positive control for cytoprotection. **A.** Analysis by western blotting of total Nrf2 (Nrf2) and phosphorylated Nrf2 (P-Nrf2); β -actin was used as the loading control. **B.** Analysis of Nrf2, NQO1 and HMOX-1 expression by RT-qPCR; the role played by the PI3-K / Akt signaling pathway on Nrf2, NQO1 and HMOX-1 expression was also evaluated in the presence of LY-294002. Significance of the differences between control (untreated cells), and vehicle (EtOH 0.5 %)-, ALA-, EPA-, DHA-, OA-, α -toco- or 7KC-treated cells; Mann-Whitney test: * $p < 0.05$ or less. Significance of the differences between 7KC-treated cells and (7KC + (ALA, EPA, DHA, OA or α -toco))-treated cells; Mann-Whitney test: # $p < 0.05$ or less. Significance of the differences between N2a cells not treated with LY-294002, and LY-294002-treated cells; Mann-Whitney test: δ $p < 0.05$ or less.

frequently, 7KC can also induce non-oxiaptophagic types of cell death, which are however always associated with oxidative stress (Vejux et al., 2020). Depending on the cell type considered, in pharmacological and therapeutic perspectives, it is therefore required to determine the type of cell death induced by 7KC and the associated signaling pathways. Since 7KC is found at increased levels in patients with age-related diseases (cardiovascular, neurodegenerative, and ocular diseases, especially) (Zarrouk et al., 2014; Samadi et al., 2021); the involvement of this oxysterol in the pathophysiology of these frequent diseases, without efficient treatments, is widely suspected. Therefore, the identification of molecules preventing 7KC-induced cytotoxicity is an important challenge with therapeutic applications. As it is known that the Mediterranean diet, rich in polyphenols as well as ω 3 and ω 9 fatty acids, is associated with a low incidence of age-related diseases and an increase of longevity (Giuffrè and Giuffrè, 2023); it was tempting to speculate that polyphenols, ω 3 and ω 9 fatty acids could prevent 7KC-induced cytotoxicity. It was previously reported that polyphenols (*trans*-resveratrol, quercetin and apigenin) present in high amount in the Mediterranean diet were strong inhibitors of 7KC-induced-oxiaptophagy (Yammine et al., 2020). So, we ask whether ALA, EPA, DHA, and OA, found at high amounts in several Mediterranean oils (Zarrouk et al., 2019), such as olive and argan oils, and blue fishes could also have cytoprotective activities towards 7KC-induced oxiaptophagy. Under treatment of murine neuronal N2a cells with 7KC, our data show an oxiaptophagic mode of cell death, involving oxidative stress, apoptosis, and autophagy, which affects several pre-mitochondrial pathways (PI3-K / PDK-1 / Akt; GSK3 / Mcl-1), the Nrf2 status and the activity of several antioxidant enzymes. These different cytotoxic effects were strongly attenuated by ALA, EPA, DHA, OA and

α -tocopherol, and the reactivation of PI3-K and glutathione peroxidase activities by these compounds was essential in cell rescue.

Oxiaptophagy is a type of cell death associated with oxidative stress, apoptosis, and autophagy (Nury et al., 2020). The notion of autophagy was reported in 2003 on human monocyte U937 cells cultured in the presence of 7KC or β -OHC (Monier et al., 2003). Since then, this type of death has been described in the presence of other oxysterols such as 25-hydroxycholesterol, 7 α -25-dihydroxycholesterol, 5,6-epoxycholesterol and 24(S)-hydroxycholesterol on different types of normal or tumor cells of several species (Seo et al., 2023; Seo et al., 2023; Kim et al., 2022; Jaouadi et al., 2021; Nury et al., 2015) to better understand and treat diseases such as cardiovascular and neurodegenerative diseases, osteoporosis and hematological malignancies. The present study, performed on murine N2a neuronal cells, showed activation of caspases-3, -7 and -9 associated with PARP cleavage and an increase in the ratio [LC3-II / LC3-I] which are specific criteria of apoptosis and autophagy, respectively. Cell death by apoptosis was morphologically associated with nuclear condensation and/or fragmentation as well as with a drop in $\Delta\Psi_m$, and an increase in the permeability of the plasma membrane to propidium iodide, confirming the important impact of 7KC at the plasma membrane level (Lechner et al., 2022; Wnętrzak et al., 2022). This plasma membrane alteration probably favors modifications of the PI3-K/PDK1/Akt pathway as previously reported on U937 cells (Vejux et al., 2009). The decrease in phosphorylated forms of PDK1 and Akt agrees with a decrease in activity of this pre-mitochondrial signaling pathway. As PI3-K / Akt represses GSK3, and contributes in its active form to several neurodegenerative processes (Kitagishi et al., 2014; Liu and Yao, 2016), the GSK3 / Mcl-1 pathway was also studied (Inuzuka et al., 2011). This showed a decrease in the phosphorylated form of

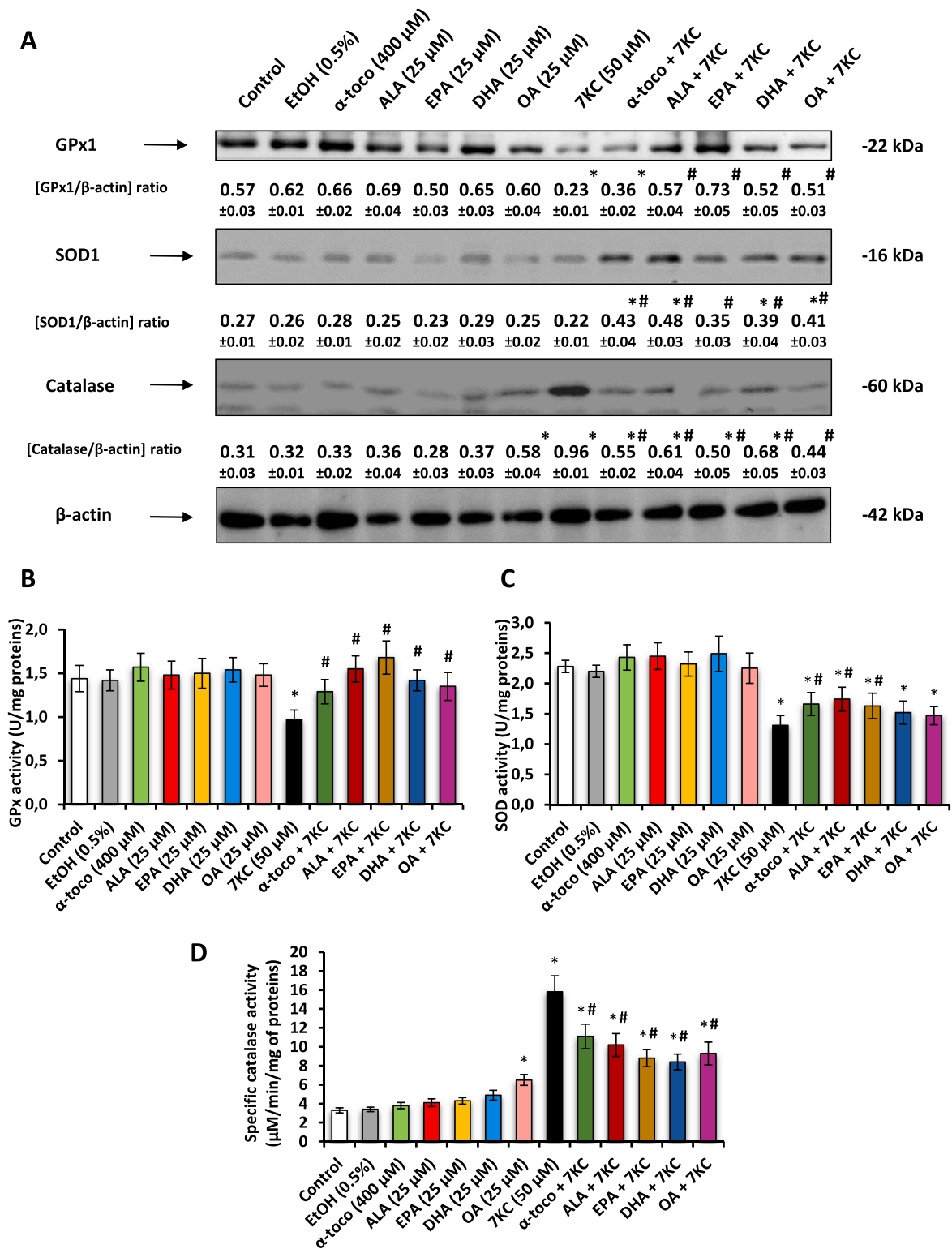
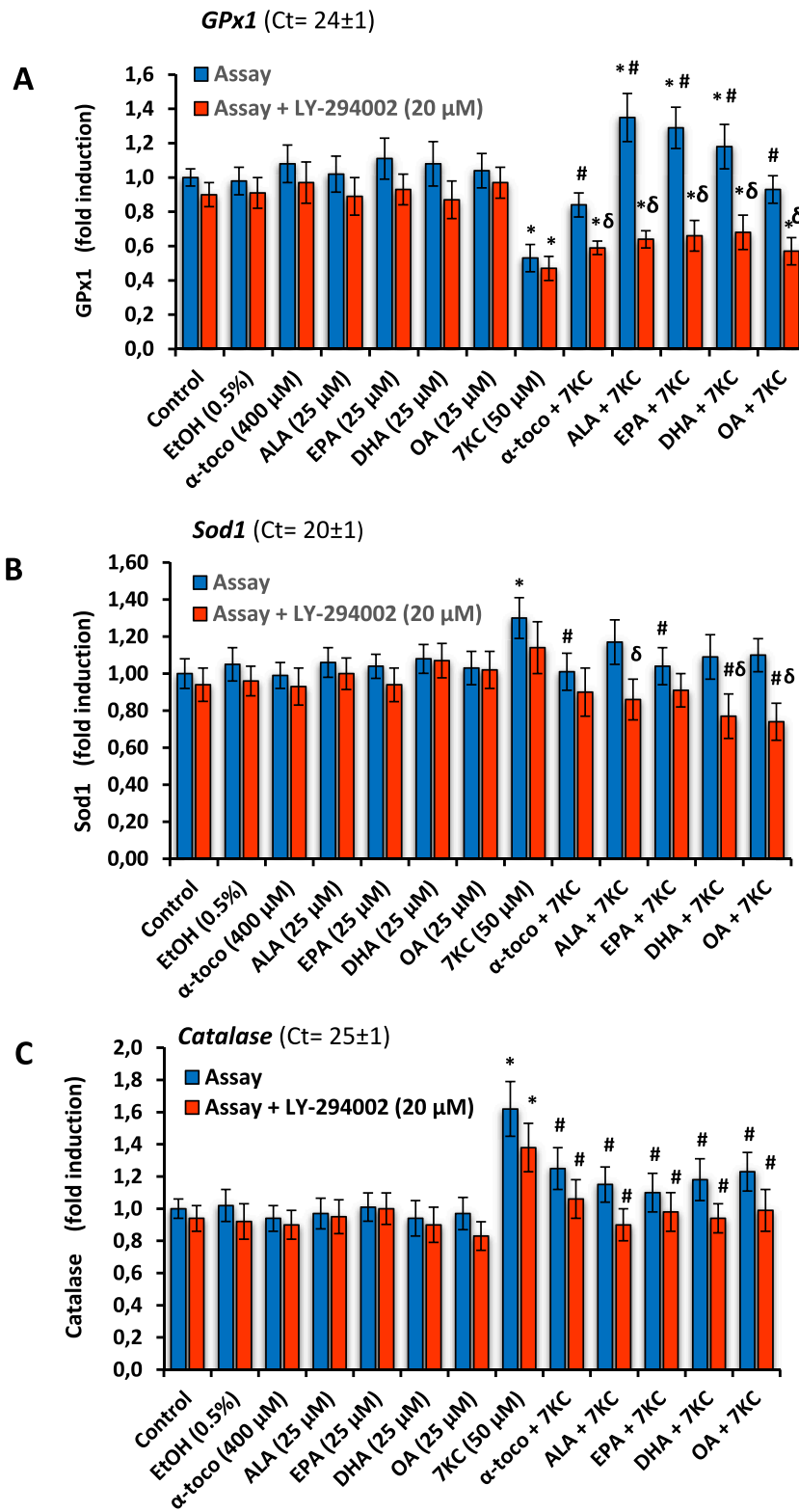


Fig. 7. Effects of 7-ketocholesterol with or without α -linolenic acid, eicosapentaenoic acid, docosahexaenoic acid, oleic acid, and α -tocopherol on the activity of glutathione peroxidase, superoxide dismutase, and catalase and on the protein level of GPx1, SOD1 and catalase. N2a cells previously cultured for 24 h were further cultured for 48 h with or without 7-ketocholesterol (7KC, 50 μ M) in the presence or absence of α -linolenic acid (ALA), eicosapentaenoic acid (EPA), docosahexaenoic acid (DHA), and oleic acid (OA) used at 25 μ M or with α -tocopherol (α -toco: 400 μ M), used as a positive control for cytoprotection. **A:** GPx1, SOD1 and catalase levels determined by Western blotting; β -actin was used as the loading control, **B:** Glutathione peroxidase (GPx), **C:** superoxide dismutase (SOD) and **D:** catalase activities; Significance of the differences between control (untreated cells), and vehicle (EtOH 0.5 %)-, ALA-, EPA-, DHA-, OA-, α -toco- or 7KC-treated cells; Mann-Whitney test: * $p < 0.05$ or less. Significance of the differences between 7KC-treated cells and (7KC + (ALA, EPA, DHA, OA or α -toco))-treated cells; Mann-Whitney test: # $p < 0.05$ or less.



(caption on next page)

Fig. 8. Effects of 7-ketocholesterol with or without α -linolenic acid, eicosapentaenoic acid, docosahexaenoic acid, oleic acid, and α -tocopherol on the expression (mRNA level) of glutathione peroxidase, superoxide dismutase, and catalase. N2a cells previously cultured for 24 h were further cultured for 48 h with or without 7-ketocholesterol (7KC, 50 μ M) in the presence or absence of α -linolenic acid (ALA), eicosapentaenoic acid (EPA), docosahexaenoic acid (DHA), and oleic acid (OA) used at 25 μ M or with α -tocopherol (α -toco: 400 μ M), used as a positive control for cytoprotection. The mRNA levels of GPx1, Sod1 and catalase were determined by RT-qPCR. LY-294002 was used as PI3-K inhibitor. Significance of the differences between control (untreated cells), and vehicle (EtOH 0.5 %)-, ALA-, EPA-, DHA-, OA-, α -toco- or 7KC-treated cells; Mann–Whitney test: * $p < 0.05$ or less. Significance of the differences between 7KC-treated cells and (7KC + (ALA, EPA, DHA, OA or α -toco))-treated cells; Mann–Whitney test: # $p < 0.05$ or less. Significance of the differences between N2a cells not treated with LY-294002, and LY-294002-treated cells; Mann–Whitney test: $\delta p < 0.05$ or less.

GSK3 in contrast to the increase observed in murine 158 N oligodendrocytes in the presence of 7KC and 7 β -OHC (Ragot et al., 2013; Ragot et al., 2011). On 158 N cells an increase in the phosphorylated form of GSK3 β , but no GSK3 α , was observed (Ragot et al., 2013; Ragot et al., 2011). However, on 158 N and N2a cells, a decrease in the level of Mcl-1 was highlighted. However, the phosphorylation state of Mcl-1, which depends on GSK3- β , conditions its degradation via the proteasome but also its interaction with the mitochondrial membrane to regulate $\Delta\Psi$ m (Ragot et al., 2013; Ragot et al., 2011). On N2a cells, as on 158 N cells, oxiaoptophagy would therefore act on the PI3-K/Akt and GSK3/Mcl-1 pathways, two pathways between which connections exist. However, when 7KC is combined with SB216763, a GSK3 inhibitor, a small and non-significant decrease in the proportion of cells with depolarized mitochondria was observed, suggesting a non-determining role of the GSK3/Mcl-1 pathway in the $\Delta\Psi$ m drop.

In addition, on N2a cells, 7KC-induced cell death was associated with oxidative stress with overproduction of ROS at the mitochondrial level but also on whole cells, which can lead to lipid peroxidation resulting in an increase in 4-HNE, a highly reactive aldehyde that can promote protein carbonylation (Grimsrud et al., 2008) and amplify the toxicity of 7KC. It is important to emphasize that the overproduction of ROS was strongly attenuated by DPI, an inhibitor of NADP(H) oxidase as reported in human smooth muscle cells in the presence of 7KC (Pedruzzi et al., 2004), which highlights that the involvement of NADP(H) oxidase could be a common feature of autophagy. However, it remains to be determined whether activated NADP(H) oxidase isoforms could vary from one cell type to another. Oxidative stress may also, at least in part, be the consequence of observed mitochondrial and peroxisomal alterations.

As the Nrf2 pathway is often activated as a response to oxidative stress (Jomova et al., 2023), this pathway has been studied on 7KC-treated N2a cells. It is indeed well described that the Nrf2 pathway activates the antioxidant response: when Nrf2 is phosphorylated, its translocation at the nuclear level activates the expression of certain antioxidant enzymes such as NQO1 and HMOX-1 (Yu and Xiao, 2021). However, under the effect of 7KC, a decrease in phosphorylated Nrf2 was observed, which is consistent with a decrease in the expression of the antioxidant enzymes NQO1 and HMOX-1. Thus, on N2a cells, 7KC strongly represses the Nrf2 pathway by inhibiting the phosphorylation of this protein, and this repression was not amplified when 7KC was combined with LY-294002, a PI3-K inhibitor, suggesting a lack of relationship between PI3-K activity and Nrf2 phosphorylation.

Moreover, during the oxidative stress induced by 7KC, the effect on some important antioxidant enzymes was variable: the expression (mRNA level) of GPx1 was greatly decreased, that of Sod1 was slightly increased and that of catalase was greatly increased. These expressions were unchanged when the 7KC was associated with LY-294002. At the protein level, the amount of GPx1 and SOD1 were decreased and that of catalase increased. In terms of enzymatic activities, those of GPx and SOD were decreased while that of catalase was increased. For SOD, at the opposite of GPx and catalase, there is therefore no relationship between mRNA and protein levels and activity. Noteworthy, our data support that these enzymatic activities play a very important role in 7KC-induced cell death. Indeed, when 7KC was combined with a catalase inhibitor (3-AT: 3-amino-1,2,4-triazole) or a GPx inhibitor (MSA: mercaptosuccinic acid), the percentage of dead cells was increased as well as the percentage of ROS overproducing cells. These effects were more pronounced in the presence of MSA than with 3-AT, suggesting

that the ability of 7KC to act on GPx is a key component in the induction of cell death and oxidative stress.

As increased 7KC-level are frequently observed in body fluids and/or tissue of patients with age-related disease, the involvement of these oxysterols in the pathophysiology of these diseases is widely suspected (Ali et al., 2022). It is therefore important to identify strategies to inactivate 7KC (esterification, sulfation, degradation) (Ghzael et al., 2022) and/or to prevent its cytotoxic activities with the use of synthetic or natural molecules, or of mixtures of molecules (Brahmi et al., 2019; Nury et al., 2021), bearing in mind that these two aspects may be closely related. As the Mediterranean diet, rich in polyphenols but also in omega-3 (ALA, EPA, DHA) and -9 (OA) acids, is known to prevent age-related diseases and is associated with an increase in longevity (Singh et al., 2022), the cytoprotective effects of the fatty acids ALA, EPA, DHA and OA have been evaluated on N2a cells treated with 7KC.

The results obtained were very significant and showed a cytoprotection of fatty acids as well as of α -tocopherol (used as a reference cytoprotective molecule) which oppose 7KC-induced oxiaoptophagy: apoptosis and autophagy are repressed, and oxidative stress was greatly reduced. Interestingly, in neuroprotection, DHA activates glutathione and thioredoxin antioxidant systems in murine hippocampal HT22 cells, including regulation of Gpx4 gene expression (Casañas-Sánchez et al., 2014; Casañas-Sánchez et al., 2015). DHA and EPA have also been shown to protect Schwann cells from oxidative stress by inducing heme oxygenase-1 (Ho-1) and catalase via Nrf-2 (Tatsumi et al., 2019). The neuroprotective effect of DHA on glutamate-induced cytotoxicity in rat hippocampal cultures was associated with increased activities of the antioxidant enzymes glutathione peroxidase and glutathione reductase (Wang et al., 2003). Cytoprotective activities of DHA and OA as well as α -tocopherol, on 7KC-induced oxiaoptophagy, have been reported on human monocytic U937 cells, murine microglial BV-2 cells and rat oligodendrocytic 158 N cells, supporting that the cytoprotective effects of this nutrients do not depend on the cell types and species (Nury et al., 2021). In the present study, ALA, EPA, DHA and OA as well as α -tocopherol, restore the PI3-K / PDK1 / Akt and GSK3 / Mcl-1 signaling pathways and strongly attenuate the degradation of Nrf2. However, when fatty acids were combined with SB216763, a GSK3 inhibitor, the cytoprotective effects were slightly reduced. On the other hand, when fatty acids (ALA, EPA, DHA, OA) and α -tocopherol were in the presence of LY-294002, which is a PI3-kinase inhibitor, the marked cytoprotective effects of these nutrients, against apoptosis (assessed by staining the nuclei with Hoechst 33342) and cell death (assessed with propidium iodide), were strongly and significantly reduced. Similarly, in the presence of LY-294002, the beneficial effects of fatty acids and α -tocopherol on the expression (mRNA level) of Nrf2, and two of its target genes (NQO1, HMOX-1) were also greatly reduced. In addition, LY-294002 also reduced the beneficial effects of fatty acids and α -tocopherol on GPx1 level. The cytoprotective effects of ALA, EPA, DHA, OA and α -tocopherol on 7KC-induced cytotoxicity via the PI3-K / PDK1 / Akt signaling pathway is therefore crucial. These data also demonstrate that the prevention of oxiaoptophagy by ALA, EPA, DHA, OA and α -tocopherol requires an attenuation of oxidative stress, and that GPx1 is a key element in the cytoprotection. These results agree with those obtained on U937 cells treated with 7KC (Lizard et al., 1998): in the presence of reduced glutathione as well as N-acetylcysteine (a precursor of glutathione), apoptosis was greatly reduced as well as oxidative stress (overproduction of ROS and lipid peroxidation). The importance of

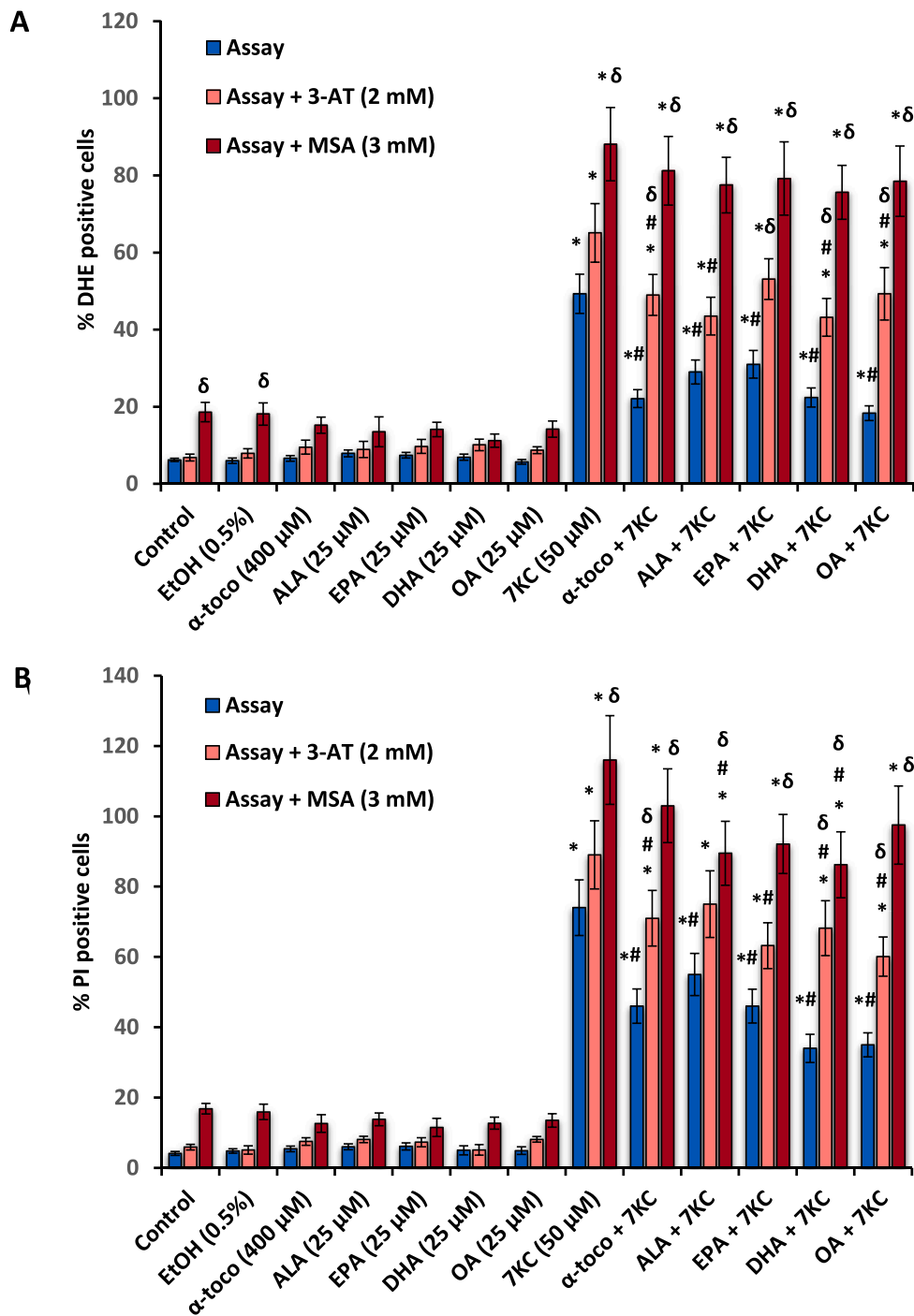


Fig. 9. Evaluation of the importance of catalase and glutathione peroxidase in 7-ketocholesterol-induced reactive oxygen species overproduction and cell death, and on the cytoprotective effects of α -linolenic acid, eicosapentaenoic acid, docosahexaenoic acid, oleic acid and α -tocopherol. N2a cells previously cultured for 24 h were further cultured for 48 h with or without 7-ketocholesterol (7KC, 50 μ M) in the presence or absence of α -linolenic acid (ALA), eicosapentaenoic acid (EPA), docosahexaenoic acid (DHA), and oleic acid (OA) used at 25 μ M or with α -tocopherol (α -toco: 400 μ M), used as a positive control for cytoprotection. The contribution of catalase and glutathione peroxidase in cell rescue (7KC-induced ROS overproduction and cell death) and on the cytoprotective effects of α -linolenic acid, eicosapentaenoic acid, docosahexaenoic acid, oleic acid and α -tocopherol were evaluated with the enzymatic inhibitors 3-aminotriazole (3-AT) for catalase; mercaptosuccinic acid (MSA) for GPx. Significance of the differences between control (untreated cells), and vehicle (EtOH 0.5 %)-, ALA-, EPA-, DHA-, OA-, α -toco- or 7KC-treated cells; Mann–Whitney test: * $p < 0.05$ or less. Significance of the differences between 7KC-treated cells and (7KC + (ALA, EPA, DHA, OA or α -toco))-treated cells; Mann–Whitney test: # $p < 0.05$ or less. Significance of the differences between cells not treated with 3-AT and MSA and 3-AT or MSA-treated cells; Mann–Whitney test: δ $p < 0.05$ or less. 3-AT: 3-Amino-1, 2, 4-triazole (Catalase inhibitor). MSA: mercaptosuccinic acid (GPx inhibitor).

restoring glutathione peroxidase activity in the cytoprotective activities of fatty acids (ALA, EPA, DHA, OA) and α -tocopherol vis-à-vis 7KC was confirmed when these nutrients were combined with mercaptosuccinic acid (MSA), a GPx inhibitor: indeed, under these conditions, the cytoprotection against oxidative stress and cell death was strongly reduced. Thus, restoring GPx activity is also an essential element for the cytoprotection against 7KC-induced cytotoxicity.

In conclusion, on neuronal murine N2a cells, 7KC induces a mode of cell death by oxiaoptophagy. This type of death is counteracted by fatty acids (ALA, EPA, DHA, OA) and α -tocopherol. These nutrients, which are very present in the Mediterranean diet, prevent mitochondrial and peroxisomal structural changes. The cytoprotection exerted by these structurally different nutrients requires a reactivation of the pre-mitochondrial pathway PI3-K / PDK-1 / Akt localized at the plasma membrane level as well as of GPx enzyme activity. These results confirm the interest of a nutritherapy based on the use of nutrients present in the Mediterranean diet. In the context of aging and age-related diseases, where increases in 7KC are often observed, acting on the PI3-K/PDK-1/Akt pathway and on GPx could pave the way for new therapeutic approaches. Setting up a high screening outpout procedure targeting the PI3-K / PDK-1 / Akt pathway and the GPx enzyme activity (GPx1 oriented) could open new perspectives in geriatric pharmacology.

Funding

This work was funded by Université de Bourgogne Franche-Comté (UBFC, Dijon, France) and the Lebanese University, Lebanon. Aline Yammine was the winner of the 2019 Mediterranean Nutrition and Health Association Prize (Arbois, France); scientific price from the NMS (Nutrition Méditerranéenne & Santé) Association.

CRediT authorship contribution statement

Aline Yammine: Investigation. **Imen Ghzaïel:** Investigation. **Vivien Pires:** Investigation. **Amira Zarrouk:** Writing – review & editing. **Omar Kharoubi:** Writing – review & editing. **Hélène Greïge-Gerges:** Supervision. **Lizette Auezova:** Supervision. **Gérard Lizard:** Conceptualization, Funding acquisition, Methodology, Project administration, Supervision, Visualization, Writing – original draft. **Anne Vejux:** Supervision, Visualization, Writing – original draft.

Declaration of competing interest

The authors declare that they have no known competing financial interests or personal relationships that could have appeared to influence the work reported in this paper.

Data availability

Data will be made available on request.

Acknowledgements

The authors also thank the “Association Méditerranéenne de Biogérontologie” (AMeBio, Président Dr Gérard Lizard) which permits interactions between researchers in gerontology and geriatrics, and ABASIM (Association Bourguignonne pour les Applications des Sciences de l'Information en Médecine; Dijon, France) for its financial supports for the students.

Appendix A. Supplementary data

Supplementary data to this article can be found online at <https://doi.org/10.1016/j.crtox.2024.100153>.

References

- Ali, J., Aziz, M.A., Rashid, M.M.O., Basher, M.A., Islam, M.S., 2022. Propagation of age-related diseases due to the changes of lipid peroxide and antioxidant levels in elderly people: a narrative review. *Health Sci Rep* 5, e650.
- Anderson, A., Campo, A., Fulton, E., Corwin, A., Jerome, W.G., O'Connor, M.S., 2020. 7-Ketocholesterol in disease and aging. *Redox Biol* 29, 101380 <https://doi.org/10.1016/j.redox.2019.101380>.
- Boselli, E., Velazco, V., Caboni, M.F., Lercker, G., 2001. Pressurized liquid extraction of lipids for the determination of oxysterols in egg-containing food. *J. Chromatogr. A* 917, 239–244. [https://doi.org/10.1016/S0021-9673\(01\)00688-4](https://doi.org/10.1016/S0021-9673(01)00688-4).
- Brahmi, F., Vejux, A., Sghaier, R., Zarrouk, A., Nury, T., Meddeb, W., Rezig, L., Namsi, A., Sassi, K., Yammine, A., Badreddine, I., Vandier-Fasseur, D., Madani, K., Boulekbache-Makhlouf, L., Nasser, B., Lizard, G., 2019. Prevention of 7-ketocholesterol-induced side effects by natural compounds. *Crit. Rev. Food Sci. Nutr* 59, 3179–3198. <https://doi.org/10.1080/10408398.2018.1491828>.
- Brzeska, M., Szymczyk, K., Sztark, A., 2016. Current knowledge about oxysterols: a review. *J. Food Sci* 81, R2299–R2308. <https://doi.org/10.1111/1750-3841.13423>.
- Casañas-Sánchez, V., Pérez, J.A., Fabelo, N., Herrera-Herrera, A.V., Fernández, C., Marín, R., González-Montelongo, M.C., Díaz, M., 2014. Addition of docosahexaenoic acid, but not arachidonic acid, activates glutathione and thioredoxin antioxidant systems in murine hippocampal HT22 cells: potential implications in neuroprotection. *J. Neurochem* 131, 470–483. <https://doi.org/10.1111/jnc.12833>.
- Casañas-Sánchez, V., Pérez, J.A., Fabelo, N., Quinto-Aleman, D., Díaz, M.L., 2015. Docosahexaenoic (DHA) modulates phospholipid-hydroperoxide glutathione peroxidase (GPx4) gene expression to ensure self-protection from oxidative damage in hippocampal cells. *Front. Physiol* 6, 203. <https://doi.org/10.3389/fphys.2015.00203>.
- Choroszyński, M., Barcikowska, M., Barczak, A., 2022. Metabolism and the effect of animal-derived oxysterols in the diet on the development of Alzheimer's disease. *Ann. Nutr. Metab* 78, 125–132. <https://doi.org/10.1159/000520514>.
- Debbabi, M., Nury, T., Helali, I., Karym, E.M., Geillon, F., Gondcaille, C., Trompier, D., Najid, A., Terreau, S., Bezine, M., Zarrouk, A., Vejux, A., Andreoletti, P., Cherkaoui-Malki, M., Savary, S., Lizard, G., 2017. Flow cytometric analysis of the expression pattern of peroxisomal proteins, Abcd1, Abcd2, and Abcd3 in BV-2 murine microglial cells. *Methods Mol. Biol* 1595, 257–265. https://doi.org/10.1007/978-1-4939-6937-1_25.
- Debbabi, M., Zarrouk, A., Bezine, M., Meddeb, W., Nury, T., Badreddine, A., Karym, E. M., Sghaier, R., Bretillon, L., Guyot, S., Samadi, M., Cherkaoui-Malki, M., Nasser, B., Mejri, M., Ben-Hammou, S., Hammami, M., Lizard, G., 2017. Comparison of the effects of major fatty acids present in the Mediterranean diet (oleic acid, docosahexaenoic acid) and in hydrogenated oils (elaidic acid) on 7-ketocholesterol-induced oxiaoptophagy in microglial BV-2 cells. *Chem. Phys. Lipids* 207, 151–170. <https://doi.org/10.1016/j.chemphyslip.2017.04.002>.
- Duda, P., Wiśniewski, J., Wójtowicz, T., Wójcicka, O., Jaśkiewicz, M., Drulis-Fajdzal, D., Rakus, D., Mucubrey, J.A., Gizak, A., 2018. Targeting GSK3 signaling as a potential therapy of neurodegenerative diseases and aging. *Expert Opin. Ther. Targets* 22, 833–848. <https://doi.org/10.1080/14728222.2018.1526925>.
- Gargiulo, S., Gamba, P., Testa, G., Leonarduzzi, G., Poli, G., 2016. The role of oxysterols in vascular ageing. *J. Physiol* 594, 2095–2113. <https://doi.org/10.1113/JP271168>.
- Ghzaïel, S., Khouloud, A.Z., Ghosh, S., Dias, I.H.K., Nury, T., Ksila, et al., Sources of 7-ketocholesterol, metabolism and inactivation strategies: food and biomedical applications, *Redox Experimental Medicine*. Volume 2022: Issue 1 (n.d.) R40–R56.
- Ghzaïel, I., Zarrouk, A., Essadek, S., Martine, L., Hammouda, S., Yammine, A., Ksila, M., Nury, T., Meddeb, W., Tahri Joutey, M., Mihoubi, W., Caccia, C., Leoni, V., Samadi, M., Acar, N., Andreoletti, P., Hammami, S., Ghraïri, T., Vejux, A., Hammami, M., Lizard, G., 2022. Protective effects of milk thistle (*Silybum marianum*) seed oil and α -tocopherol against 7 β -hydroxycholesterol-induced peroxisomal alterations in murine C2C12 myoblasts: Nutritional insights associated with the concept of pexotherapy. *Steroids* 183, 109032. <https://doi.org/10.1016/j.steroids.2022.109032>.
- Ghzaïel, I., Zarrouk, A., Pires, V., de Barros, J.-P.-P., Hammami, S., Ksila, M., Hammami, M., Ghraïri, T., Jouanny, P., Vejux, A., Lizard, G., 2023. 7 β -Hydroxycholesterol and 7-ketocholesterol: New oxidative stress biomarkers of sarcopenia inducing cytotoxic effects on myoblasts and myotubes. *J. Steroid Biochem. Mol. Biol* 232, 106345 <https://doi.org/10.1016/j.jsmb.2023.106345>.
- Giuffrè, D., Giuffrè, A.M., 2023. Mediterranean diet and health in the elderly. *AIMS Public Health* 10, 568–576. <https://doi.org/10.3934/publichealth.2023040>.
- Griffiths, W.J., Abdel-Khalik, J., Moore, S.F., Wijeyekoon, R.S., Crick, P.J., Yutuc, E., Farrell, K., Breen, D.P., Williams-Gray, C.H., Theofilopoulos, S., Arenas, E., Trupp, M., Barker, R.A., Wang, Y., 2021. The cerebrospinal fluid profile of cholesterol metabolites in parkinson's disease and their association with disease state and clinical features. accessed March 21, 2023 *Front. Aging Neurosci* 13. <https://doi.org/10.3389/fnagi.2021.685594>.
- Grimsrud, P.A., Xie, H., Griffin, T.J., Bernholz, D.A., 2008. Oxidative stress and covalent modification of protein with bioactive aldehydes. *J. Biol. Chem* 283, 21837–21841. <https://doi.org/10.1074/jbc.R700019200>.
- Inuzuka, H., Fukushima, H., Shaik, S., Liu, P., Lau, A.W., Wei, W., 2011. Mcl-1 ubiquitination and destruction. *Oncotarget* 2, 239–244. <https://doi.org/10.18632/oncotarget.242>.
- Jaouadi, O., Limam, I., Abdelkarim, M., Berred, E., Chahbi, A., Caillot, M., Sola, B., Ben Aissa-Fennira, F., 2021. 5,6-epoxycholesterol isomers induce oxiaoptophagy in myeloma cells. *Cancers (basel)* 13, 3747. <https://doi.org/10.3390/cancers13153747>.
- Jomova, K., Raptova, R., Alomar, S.Y., Alwasel, S.H., Nepovimova, E., Kuca, K., Valko, M., 2023. Reactive oxygen species, toxicity, oxidative stress, and

- antioxidants: chronic diseases and aging. *Arch. Toxicol.* 97, 2499–2574. <https://doi.org/10.1007/s00204-023-03562-9>.
- Kamiloglu, S., Sari, G., Ozdal, T., Capanoglu, E., 2020. Guidelines for cell viability assays. *Food Frontiers*. 1, 332–349. <https://doi.org/10.1002/fft2.44>.
- Kim, J.-S., Lim, H., Seo, J.-Y., Kang, K.-R., Yu, S.-K., Kim, C.S., Kim, D.K., Kim, H.-J., Seo, Y.-S., Lee, G.-J., You, J.-S., Oh, J.-S., 2022. GPR183 regulates α ,25-dihydroxycholesterol-induced oxiaoptophagy in L929 mouse fibroblast cell. *Molecules* 27, 4798. <https://doi.org/10.3390/molecules27154798>.
- Kitagishi, Y., Nakanishi, A., Ogura, Y., Matsuda, S., 2014. Dietary regulation of PI3K/AKT/GSK-3 β pathway in Alzheimer's disease. *Alzheimers Res. Ther.* 6, 35. <https://doi.org/10.1186/alzrt265>.
- Ksila, M., Ghzaïel, I., Pires, V., Ghraïri, T., Masmoudi-Kouki, O., Latruffe, N., Vervandier-Fasseur, D., Vejux, A., Lizard, G., 2023. Characterization of cell death induced by imine analogs of trans-resveratrol: induction of mitochondrial dysfunction and overproduction of reactive oxygen species leading to, or not apoptosis without the increase in the S-phase of the cell cycle. *Molecules*. 28, 3178. <https://doi.org/10.3390/molecules28073178>.
- Lechner, B.-D., Smith, P., McGill, B., Marshall, S., Trick, J.L., Chumakov, A.P., Winlove, C.P., Konovalov, O.V., Lorenz, C.D., Petrov, P.G., 2022. The effects of cholesterol oxidation on erythrocyte plasma membranes: a monolayer study. *Membranes (basel)*. 12, 828. <https://doi.org/10.3390/membranes12090828>.
- Leonarduzzi, G., Sottero, B., Poli, G., 2002. Oxidized products of cholesterol: dietary and metabolic origin, and proatherosclerotic effects (review). *J. Nutr. Biochem.* 13, 700–710. [https://doi.org/10.1016/s0955-2863\(02\)00222-x](https://doi.org/10.1016/s0955-2863(02)00222-x).
- Leoni, V., Caccia, C., 2013. 24S-hydroxycholesterol in plasma: a marker of cholesterol turnover in neurodegenerative diseases. *Biochimie* 95, 595–612. <https://doi.org/10.1016/j.biochi.2012.09.025>.
- Letai, A., 2006. Growth factor withdrawal and apoptosis: the middle game. *Mol. Cell* 21, 728–730. <https://doi.org/10.1016/j.molcel.2006.03.005>.
- Liu, X., Yao, Z., 2016. Chronic over-nutrition and dysregulation of GSK3 in diseases. *Nutr. Metab. (Lond.)* 13, 49. <https://doi.org/10.1186/s12986-016-0108-8>.
- Lizard, G., Fournel, S., Genestier, L., Dhedin, N., Chaput, C., Flacher, M., Mutin, M., Panaye, G., Revillard, J.P., 1995. Kinetics of plasma membrane and mitochondrial alterations in cells undergoing apoptosis. *Cytometry* 21, 275–283. <https://doi.org/10.1002/cyto.990210308>.
- Lizard, G., Gueldry, S., Sordet, O., Monier, S., Athias, A., Miguet, C., Bessede, G., Lemaire, S., Solary, E., Gambert, P., 1998. Glutathione is implied in the control of 7-ketocholesterol-induced apoptosis, which is associated with radical oxygen species production. *FASEB J.* 12, 1651–1663. <https://doi.org/10.1096/ajpcell.12.15.1651>.
- Mahalakshmi, K., Parimalanandhini, D., Sangeetha, R., Livya Catherine, M., Beulaja, M., Thiagarajan, R., Arumugam, M., Janarthanan, S., Manikandan, R., 2021. Influential role of 7-Ketocholesterol in the progression of Alzheimer's disease. *Prostaglandins Other Lipid Mediat.* 156, 106582. <https://doi.org/10.1016/j.prostaglandins.2021.106582>.
- Malvitte, L., Montange, T., Joffre, C., Vejux, A., Maïza, C., Bron, A., Creuzot-Garcher, C., Lizard, G., 2006. Analogies between atherosclerosis and age-related maculopathy: expected roles of oxysterols. *J. Fr. Ophtalmol.* 29, 570–578. [https://doi.org/10.1016/s0181-5512\(06\)73815-3](https://doi.org/10.1016/s0181-5512(06)73815-3).
- Manning, B.D., Toker, A., 2017. AKT/PKB signaling: navigating the network. *Cell* 169, 381–405. <https://doi.org/10.1016/j.cell.2017.04.001>.
- Martelli, A.M., Faenza, I., Billi, A.M., Manzoli, L., Evangelisti, C., Falà, F., Cocco, L., 2006. Intranuclear 3'-phosphoinositide metabolism and Akt signaling: new mechanisms for tumorigenesis and protection against apoptosis? *Cell. Signal.* 18, 1101–1107. <https://doi.org/10.1016/j.cellsig.2006.01.011>.
- McComb, M., Browne, R.W., Bhattacharya, S., Bodziak, M.L., Jakimovski, D., Weinstock-Guttman, B., Kuhle, J., Zivadinov, R., Ramanathan, M., 2021. The cholesterol oxidation products, 7-ketocholesterol and 7 β -hydroxycholesterol are associated with serum neurofilaments in multiple sclerosis. *Mult. Scler. Relat. Disord.* 50, 102864. <https://doi.org/10.1016/j.msard.2021.102864>.
- Milkovic, L., Zarkovic, N., Marusic, Z., Zarkovic, K., Jaganjac, M., 2023. The 4-hydroxynonenal-protein adducts and their biological relevance: are some proteins preferred targets? *Antioxidants (basel)*. 12, 856. <https://doi.org/10.3390/antiox12040856>.
- Monier, S., Samadi, M., Prunet, C., Denance, M., Laubriet, A., Athias, A., Berthier, A., Steinmetz, E., Jürgens, G., Nègre-Salvayre, A., Bessède, G., Lemaire-Ewing, S., Néel, D., Gambert, P., Lizard, G., 2003. Impairment of the cytotoxic and oxidative activities of 7 beta-hydroxycholesterol and 7-ketocholesterol by esterification with oleate. *Biochem. Biophys. Res. Commun.* 303, 814–824. [https://doi.org/10.1016/s0006-291x\(03\)00412-1](https://doi.org/10.1016/s0006-291x(03)00412-1).
- Mu, Y., Maharjan, Y., Kumar Dutta, R., Wei, X., Kim, J.H., Son, J., Park, C., Park, R., 2021. Pharmacological inhibition of catalase induces peroxisome leakage and suppression of LPS induced inflammatory response in Raw 264.7 cell. *PLoS One* 16, e0245799.
- Mutemberezi, V., Guillemot-Legrès, O., Muccioli, G.G., 2016. Oxysterols: from cholesterol metabolites to key mediators. *Prog. Lipid Res.* 64, 152–169. <https://doi.org/10.1016/j.plipres.2016.09.002>.
- Nury, T., Zarrouk, A., Mackrill, J.J., Samadi, M., Durand, P., Riedinger, J.-M., Doria, M., Vejux, A., Limagne, E., Delmas, D., Prost, M., Moreau, T., Hammami, M., Delage-Mourroux, R., O'Brien, N.M., Lizard, G., 2015. Induction of oxiaoptophagy on 158N murine oligodendrocytes treated by 7-ketocholesterol-, 7 β -hydroxycholesterol-, or 24(S)-hydroxycholesterol: Protective effects of α -tocopherol and docosahexaenoic acid (DHA; C22:6 n-3). *Steroids* 99, 194–203. <https://doi.org/10.1016/j.steroids.2015.02.003>.
- Nury, T., Zarrouk, A., Ragot, K., Debbabi, M., Riedinger, J.-M., Vejux, A., Aubourg, P., Lizard, G., 2017. 7-Ketocholesterol is increased in the plasma of X-ALD patients and induces peroxisomal modifications in microglial cells: Potential roles of 7-ketocholesterol in the pathophysiology of X-ALD. *J. Steroid Biochem. Mol. Biol.* 169, 123–136. <https://doi.org/10.1016/j.jsbmb.2016.03.037>.
- Nury, T., Zarrouk, A., Yammine, A., Mackrill, J.J., Vejux, A., Lizard, G., 2020. Oxiaoptophagy: a type of cell death induced by some oxysterols. *Br. J. Pharmacol.* <https://doi.org/10.1111/bph.15173>.
- Nury, T., Zarrouk, A., Yammine, A., Mackrill, J.J., Vejux, A., Lizard, G., 2021. Oxiaoptophagy: a type of cell death induced by some oxysterols. *Br. J. Pharmacol.* 178, 3115–3123. <https://doi.org/10.1111/bph.15173>.
- Nury, T., Yammine, A., Ghzaïel, I., Sassi, K., Zarrouk, A., Brahm, F., Samadi, M., Rup-Jacques, S., Vervandier-Fasseur, D., Pais de Barros, J.P., Bergas, V., Ghosh, S., Majeed, M., Pande, A., Atanasov, A., Hammami, S., Hammami, M., Mackrill, J., Nasser, B., Andreoletti, P., Cherkaoui-Malki, M., Vejux, A., Lizard, G., 2021. Attenuation of 7-ketocholesterol- and 7 β -hydroxycholesterol-induced oxiaoptophagy by nutrients, synthetic molecules and oils: potential for the prevention of age-related diseases. *Ageing Res. Rev.* 68, 101324. <https://doi.org/10.1016/j.arr.2021.101324>.
- Pedrucci, E., Guichard, C., Ollivier, V., Driss, F., Fay, M., Prunet, C., Marie, J.-C., Pouzet, C., Samadi, M., Elbim, C., 2004. NAD(P)H oxidase Nox-4 mediates 7-ketocholesterol-induced endoplasmic reticulum stress and apoptosis in human aortic smooth muscle cells. *Mol. Cell Biol.* 24, 10703–10717. <https://doi.org/10.1128/MCB.24.24.10703-10717.2004>.
- Poli, G., Biasi, F., Leonarduzzi, G., 2013. Oxysterols in the pathogenesis of major chronic diseases. *Redox Biol.* 1, 125–130. <https://doi.org/10.1016/j.redox.2012.12.001>.
- Poli, G., Leoni, V., Biasi, F., Canzoneri, F., Risso, D., Menta, R., 2022. Oxysterols: from redox bench to industry. *Redox Biol.* 49, 102220. <https://doi.org/10.1016/j.redox.2021.102220>.
- Przygowski, K., Jelen, H., Wasowicz, E., 2000. Determination of cholesterol oxidation products in milk powder and infant formulas by gas chromatography and mass spectrometry. *Nahrung* 44, 122–125. [https://doi.org/10.1002/\(SICI\)1521-3803\(20000301\)44:2<122::AID-FOOD122>3.0.CO;2-R](https://doi.org/10.1002/(SICI)1521-3803(20000301)44:2<122::AID-FOOD122>3.0.CO;2-R).
- Quispe, R.L., Canto, R.F.S., Jaramillo, M.L., Barbosa, F.A.R., Braga, A.L., de Bem, A.F., Farina, M., 2018. Design, synthesis, and in vitro evaluation of a novel probockal derivative: protective activity in neuronal cells through GPx upregulation. *Mol. Neurobiol.* 55, 7619–7634. <https://doi.org/10.1007/s12035-018-0939-6>.
- Ragot, K., Delmas, D., Athias, A., Nury, T., Baarine, M., Lizard, G., 2011. α -Tocopherol impairs 7-ketocholesterol-induced caspase-3-dependent apoptosis involving GSK-3 activation and McI-1 degradation on 158N murine oligodendrocytes. *Chem. Phys. Lipids* 164, 469–478. <https://doi.org/10.1016/j.chemphyslip.2011.04.014>.
- Ragot, K., Mackrill, J.J., Zarrouk, A., Nury, T., Aires, V., Jacquin, A., Athias, A., Pais de Barros, J.-P., Vejux, A., Riedinger, J.-M., Delmas, D., Lizard, G., 2013. Absence of correlation between oxysterol accumulation in lipid raft microdomains, calcium increase, and apoptosis induction on 158N murine oligodendrocytes. *Biochem. Pharmacol.* 86, 67–79. <https://doi.org/10.1016/j.bcp.2013.02.028>.
- Rezig, L., Ghzaïel, I., Ksila, M., Yammine, A., Nury, T., Zarrouk, A., Samadi, M., Chouaïbi, M., Vejux, A., Lizard, G., 2022. Cytoprotective activities of representative nutrients from the Mediterranean diet and of Mediterranean oils against 7-ketocholesterol- and 7 β -hydroxycholesterol-induced cytotoxicity: Application to age-related diseases and civilization diseases. *Steroids* 187, 109093. <https://doi.org/10.1016/j.steroids.2022.109093>.
- Rodríguez, I.R., Clark, M.E., Lee, J.W., Curcio, C.A., 2014. 7-ketocholesterol accumulates in ocular tissues as a consequence of aging and is present in high levels in drusen. *Exp. Eye Res.* 128, 151–155. <https://doi.org/10.1016/j.exer.2014.09.009>.
- Rodríguez, I.R., Larraye, I.M., 2010. Cholesterol oxidation in the retina: implications of 7KCh formation in chronic inflammation and age-related macular degeneration. *J. Lipid Res.* 51, 2847–2862. <https://doi.org/10.1194/jlr.R004820>.
- Sabolová, M., Pohorelá, B., Fišnar, J., Kourimská, L., Chrpová, D., Pánek, J., 2017. Formation of oxysterols during thermal processing and frozen storage of cooked minced meat. *J. Sci. Food Agric.* 97, 5092–5099. <https://doi.org/10.1002/jsfa.8386>.
- Samadi, A., Sabuncuoglu, S., Samadi, M., Isikhan, S.Y., Chirumbolo, S., Peana, M., Lay, I., Yalcinkaya, A., Björklund, G., 2021. A comprehensive review on oxysterols and related diseases. *Curr. Med. Chem.* 28, 110–136. <https://doi.org/10.2174/0929867327666200316142659>.
- V. Sandoval, H. Sanz-Lamora, G. Arias, P.F. Marrero, D. Haro, J. Relat, *Metabolic Impact of Flavonoids Consumption in Obesity*, (n.d.).
- Seo, Y.-S., Kang, K.-R., Lim, H., Seo, J.-Y., Kim, D.K., Kim, J.-S., 2023. 25-hydroxycholesterol-induced osteoblast oxiaoptophagy is involved in the pathophysiological process of osteoporosis. *In Vivo* 37, 204–217.
- Seo, J.-Y., Kim, T.-H., Kang, K.-R., Lim, H., Choi, M.-C., Kim, D.K., Chun, H.S., Kim, H.-J., Yu, S.-K., Kim, J.-S., 2023. α ,25-dihydroxycholesterol-induced oxiaoptophagic chondrocyte death via the modulation of p53-akt-mtor axis in osteoarthritis pathogenesis. *Mol. Cells* 46, 245–255. <https://doi.org/10.14348/molcells.2023.2149>.
- Singh, R.B., Fedacko, J., Fatima, G., Magomedova, A., Watanabe, S., Elkilany, G., 2022. Why and how the indo-mediterranean diet may be superior to other diets: the role of antioxidants in the diet. *Nutrients* 14, 898. <https://doi.org/10.3390/nu14040898>.
- Song, X., Long, D., 2020. Nrf2 and ferroptosis: a new research direction for neurodegenerative diseases. *Front. Neurosci.* 14, 267. <https://doi.org/10.3389/fnins.2020.00267>.
- Tatsumi, Y., Kato, A., Sango, K., Himeno, T., Kondo, M., Kato, Y., Kamiya, H., Nakamura, J., Kato, K., 2019. Omega-3 polyunsaturated fatty acids exert anti-oxidant effects through the nuclear factor (erythroid-derived 2)-related factor 2 pathway in immortalized mouse Schwann cells. *J. Diabetes Investig.* 10, 602–612. <https://doi.org/10.1111/jdi.12931>.
- Vejux, A., Guyot, S., Montange, T., Riedinger, J.-M., Kahn, E., Lizard, G., 2009. Phospholipidosis and down-regulation of the PI3-K/PDK-1/Akt signalling pathway are vitamin E inhibitable events associated with 7-ketocholesterol-induced

- apoptosis. *J. Nutr. Biochem.* 20, 45–61. <https://doi.org/10.1016/j.jnutbio.2007.12.001>.
- Vejux, A., Abed-Vieillard, D., Hajji, K., Zarrouk, A., Mackrill, J.J., Ghosh, S., Nury, T., Yammine, A., Zaibi, M., Mihoubi, W., Bouchab, H., Nasser, B., Grosjean, Y., Lizard, G., 2020. 7-Ketocholesterol and 7 β -hydroxycholesterol: In vitro and animal models used to characterize their activities and to identify molecules preventing their toxicity. *Biochem. Pharmacol.* 173, 113648 <https://doi.org/10.1016/j.bcp.2019.113648>.
- Wang, M., Long, W., Li, D., Wang, D., Zhong, Y., Mu, D., Song, J., Xia, M., 2017. Plasma 7-ketocholesterol levels and the risk of incident cardiovascular events. *Heart* 103, 1788–1794. <https://doi.org/10.1136/heartjnl-2016-310914>.
- Wang, R., Xia, L., Gabrilove, J., Waxman, S., Jing, Y., 2013. Downregulation of Mcl-1 through GSK-3 β activation contributes to arsenic trioxide-induced apoptosis in acute myeloid leukemia cells. *Leukemia* 27, 315–324. <https://doi.org/10.1038/leu.2012.180>.
- Wang, X., Zhao, X., Mao, Z.-Y., Wang, X.-M., Liu, Z.-L., 2003. Neuroprotective effect of docosahexaenoic acid on glutamate-induced cytotoxicity in rat hippocampal cultures. *Neuroreport* 14, 2457–2461. <https://doi.org/10.1097/00001756-200312190-00033>.
- Wnietrzak, A., Chachaj-Brekiesz, A., Stepniak, A., Kobierski, J., Dynarowicz-Latka, P., 2022. Different effects of oxysterols on a model lipid raft - Langmuir monolayer study complemented with theoretical calculations. *Chem. Phys. Lipids* 244, 105182. <https://doi.org/10.1016/j.chemphyslip.2022.105182>.
- Yammine, A., Nury, T., Vejux, A., Latruffe, N., Vervandier-Fasseur, D., Samadi, M., Greige-Gerges, H., Auezova, L., Lizard, G., 2020. Prevention of 7-ketocholesterol-induced overproduction of reactive oxygen species, mitochondrial dysfunction and cell death with major nutrients (polyphenols, ω 3 and ω 9 unsaturated fatty acids) of the mediterranean diet on N2a neuronal cells. *Molecules* 25, E2296. <https://doi.org/10.3390/molecules25102296>.
- Yan, P.S., 1999. Cholesterol oxidation products. Their occurrence and detection in our foodstuffs. *Adv Exp Med Biol.* 459, 79–98.
- Yeh, C.J., Hsi, B.L., Faulk, W.P., 1981. Propidium iodide as a nuclear marker in immunofluorescence. II. Use with cellular identification and viability studies. *J. Immunol. Methods* 43, 269–275. [https://doi.org/10.1016/0022-1759\(81\)90174-5](https://doi.org/10.1016/0022-1759(81)90174-5).
- Yu, C., Xiao, J.-H., 2021. The keap1-Nrf2 system: a mediator between oxidative stress and aging. *Oxid. Med. Cell. Longev.* 2021, 6635460. <https://doi.org/10.1155/2021/6635460>.
- Zarrouk, A., Vejux, A., Mackrill, J., O'Callaghan, Y., Hammami, M., O'Brien, N., Lizard, G., 2014. Involvement of oxysterols in age-related diseases and ageing processes. *Ageing Res. Rev.* 18, 148–162. <https://doi.org/10.1016/j.arr.2014.09.006>.
- Zarrouk, A., Nury, T., Samadi, M., O'Callaghan, Y., Hammami, M., O'Brien, N.M., Lizard, G., Mackrill, J.J., 2015. Effects of cholesterol oxides on cell death induction and calcium increase in human neuronal cells (SK-N-BE) and evaluation of the protective effects of docosahexaenoic acid (DHA; C22:6 n-3). *Steroids* 99, 238–247. <https://doi.org/10.1016/j.steroids.2015.01.018>.
- Zarrouk, A., Martine, L., Grégoire, S., Nury, T., Meddeb, W., Camus, E., Badreddine, A., Durand, P., Namsi, A., Yammine, A., Nasser, B., Mejri, M., Bretillon, L., Mackrill, J.J., Cherkaoui-Malki, M., Hammami, M., Lizard, G., 2019. Profile of fatty acids, tocopherols, phytosterols and polyphenols in mediterranean oils (argan oils, olive oils, milk thistle seed oils and nigella seed oil) and evaluation of their antioxidant and cytoprotective activities. *Curr. Pharm. Des.* 25, 1791–1805. <https://doi.org/10.2174/1381612825666190705192902>.